THESIS

GROUND-TRUTHING VEGETATION INDICES AND MODELS IN NORTHERN COLORADO RANGELANDS

Submitted By

Cassidy Behnke

Graduate Degree Program in Ecology

In partial fulfillment of the requirements

For the Degree of Master of Science

Colorado State University

Fort Collins, Colorado

Fall 2025

Master's Committee:

Advisor: Troy Ocheltree

Wade Tinkham

Jane Stewart

Lauren Porensky

ABSTRACT

GROUND-TRUTHING VEGETATION INDICES AND MODELS IN NORTHERN COLORADO RANGELANDS

The sustainable management of rangeland ecosystems is becoming more challenging than ever with the increasing variation in climate patterns occurring across the globe. Rangelands are integral to the production of livestock and account for approximately 30% of land area in the United States. To the rangeland stakeholders who depend on these landscapes to produce forage for grazing livestock, longer periods of drought and intense summer heat are growing concerns. Adaptive rangeland management can help bring resilience to these working ecosystems but requires that pastures be constantly monitored in order to inform adjustments to management actions. Advancements in the application of novel technologies, such as remotely-captured imagery, can give rangeland managers this needed up-to-date insight into the health of vegetation in their pastures. A variety of spectral indices and biomass models, made from remotely-captured imagery, have been shown to correlate with forage conditions in grassland ecosystems with mixed success, but few have been tested in Northern Colorado's semi-arid grasslands under drought. Thus, the goal of my project is to investigate the application of vegetation indices in predicting forage conditions in a semi-arid ecosystem over the course of an irregularly dry growing season.

AKNOWLEDGEMENTS

This project would have been entirely impossible without the combined effort of the Ocheltree Lab, the project drone pilot, my committee members, and my family. Firstly, I thank my advisor, Troy Ocheltree, for having the patience and time to take me on for this project and leading me through to its belated completion. I thank Seton Bachle, Dan Spitzer, Scott Bradfield, Zoe Lipscomb, and Anna Wright of the Ocheltree Lab each for sharing time out of their summer to help with this project, either in preparing acres of pasture for the study, collecting field samples by the dozen, or weighing dried samples back in our lab. That time was in high demand for us all, and I have so much appreciation for that collective aid in my hours of need. I also thank Lauren Lad, the dedicated drone pilot on this project, for the hours spent in the field collecting imagery and later, processing integral data for this project. I also thank my committee members for bearing with me through the ups and downs of this project and offering much needed insights to the research process. And finally thank you to my family and partner for their unwavering support of this endeavor. I am beyond grateful to everyone for taking part in this research; I could not have gotten here without you.

TABLE OF CONTENTS

CHAPTER 1: ADAPTIVE RANGELAND MANAGEMENT AND THE SGS

1.1 Background

Making up approximately 35% of Earth's land area, grasslands account for more terrestrial surface than any other biome (O'Mara, 2012). As such, grasslands provide key ecosystem services to societies around the globe, including carbon sequestration, climate moderation, wildlife habitat, and human agriculture (Lauenroth and Sala, 1992; Joyce at al. 2001). The single most expansive stretch of grasslands in North America, a region known as the Great Plains, is integral to industrial agriculture for producing both meats and crops (Lauenroth and Burke, 2008; Havstad et al. 2009; Blaire at al. 2014). In fact, the Great Plains contains more than half of the United States' dryland grazing pastures, otherwise known as rangelands (Bigelow and Borchers, 2017). These working ecosystems are characterized by native and naturalized vegetation, poor soils, low precipitation, and high spatial variability in plant production, rendering rangeland management here exceptionally complex (Havstad et al. 2007; Moore et al. 2015). Indeed, the growing potential for climatic crises in the coming decades threatens the ecological stability of our grassland ecosystems, and thus threatens our capacity to produce food for the growing global population (Kukal and Irmak, 2017; Briske at al. 2021; IPCC, 2022). One way to combat this threat is through the continuous adaptation of the management techniques we utilize when stewarding these systems (Derner and Augustine, 2016; McCollum at al. 2017; Jones et al. 2021). By studying the dynamics of our rangeland ecosystems and the ever-advancing methods with which we monitor them, I intend to inform adaptive rangeland management methods to increase the resilience of our rangeland ecosystems as well as the agricultural industries they support.

1.1.1 The Shortgrass Steppe Region

Within the Great Plains, there exists a variety of grasslands; from the tallgrass prairie, to the shortgrass steppe, and the mixed prairies in between (Lauenroth and Burke, 2008). Of these grasslands, the shortgrass steppe (SGS) is commonly the warmest, driest, and least productive, and as such can prove especially challenging to manage as rangelands (Lauenroth and Milchunas, 1991). Geographically, the region accounts for the southeast section of the Great Plains region, extending from the southwest border of Nebraska through eastern Colorado and

New Mexico, the western edge of Kansas, the panhandle of Oklahoma, and south into east-central Texas. Across its extent, the SGS follows low to high gradients of North-South temperature and West-East precipitation (Lauenroth et al. 2000; Joyce et al. 2001). The mean annual temperature in the SGS historically ranges from ~9°C at the northernmost extent to ~17°C at the southernmost extent; however, daily temperatures have the potential to vary widely from dawn to midday and from season to season. The mean annual precipitation ranges from 300 to 550mm, regularly resulting in low humidity and soil moisture content in the region (Lauenroth et al. 1999). Soils are predominantly loamy and well drained, and as such, do not hold much moisture or nutrients (Lauenroth and Burke, 2008). These extreme conditions render precipitation a major driver for photosynthesis, and thus rangeland productivity (Epstein et al. 1997; McCollum et al. 2017). Indeed, widespread drought is historically common to the SGS and a regular challenge faced by rangeland managers in the region (Sala et al. 1988; Moore et al. 2015).

Plant communities in the SGS are usually dominated by perennial grasses, intermixed with various forbs and shrubs. Most plant species found in the steppe are either extraordinarily hardy to the extreme drought conditions or principally dependent on the rare incidence of rain. Native species are often adapted to the long, dry summers common to the region, and most are also relatively resistant to disturbances like drought, grazing, fire, and soil erosion (Lauenroth and Sala, 1992; Lauenroth and Burke, 2008). These species are generally short in stature, sparse in canopy, and slow to establish, such that soil is left exposed between individuals. Some native species found in the steppe are: *Bouteloua dactyloides* or Buffalograss, *Bouteloua gracilis* or Blue Grama, *Artemisia frigida* or Prairie Sagewort, *Pascopyrum smithii* or Western Wheat, and *Sphaeralcea coccinea* or Scarlett Globemallow (Ogle, 2002; Taliga and Parr, 2012; Brakie, 2013; Gucker and Shaw, 2018). Conversely, naturalized species found in the steppe are more vulnerable to disturbance than native species, but are also more readily able to utilize unseasonable precipitation events, such that, when resources are plentiful, the growth of these introduced species outpaces that of their native counterparts. Naturalized species also tend to grow more closely together and can spread to cover exposed soil more often than native species. Naturalized species common to the steppe include: *Agropyron cristatum* or Crested Wheatgrass and *Psathyrostachys junceus* or Russian Wildrye (Ogle at al. 2004; Ogle at al. 2006; Ogle at al. 2009).

Today, plant communities in the SGS contain a mix of both native and naturalized species, but the landscape has not always looked as it does now. Like much of North America, these lands have a long history of human manipulation (Lauenroth and Burke, 2008). While indigenous peoples of the region might have burned these systems or cultivated land on a family scale, the management choices most evident across the SGS today are those of 19th century settlers and the generations of farmers and ranchers that followed. With this mass immigration to the American West came large-scale crop production and cattle ranching, which contributed to the degradation of grasslands across the Great Plains (Skold, 1989; Sylvester and Gutmann, 2008). By the early 20th century, decades of soil erosion interspersed with intense droughts eventually led the United States government to establish a variety of programs focused on restoring tracts of grassland and studying how to best foster resiliency in working ecosystems, like those across the SGS. One such surviving program is the Conservation Reserve Program (CRP), a USDA program that encourages farmers to convert ecologically-sensitive lands, like arid croplands, into more resilient ecosystems, such as native grasslands or buffer strips (USDA, 2004; Cox, 2006). Through this and similar programs, much of the SGS that had been previously degraded through crop cultivation has been restored to native and naturalized species compositions like the rangeland pastures used in this study.

Rangelands account for most of the land use in the SGS. Nearly 70% of the region is now used to graze livestock, which continues the region's lengthy history of large herbivore presence (Lauenroth and Burke, 2008; National Agricultural Statistical Service, USDA, 2019). The SGS uniquely withstands the impacts of grazing, and even becomes more resilient to invasion and disturbance when moderately grazed (Axelrod, 1985; Lauenroth et al. 2000). Thus, these livestock are uniquely capable of strengthening the resilience of the SGS ecosystem (Porensky et al. 2017). When sustainably managed, cattle grazing can help maintain a biodiverse grassland community, not only by means of selective consumption, but also through vegetation trampling, soil aeration, nutrient fertilization, and seed transportation. In contrast, management that allows cattle to over- or under-graze the landscape could instead result in slowed productivity, increased invasive species spread, and overall reduced resilience of the ecosystem (Heitschmidt and Stuth, 1991; Havstad et al. 2007; Sala et al. 2017; Jones et al. 2021). The challenge of finding the most sustainable grazing patterns for rangelands in the SGS is made yet more complex in the context of increased heat-stress and drought (IPCC, 2022). The extreme conditions predicted to develop

in the SGS as a result of climate change could further limit the photosynthetic activity of vegetation found across the steppe, suppressing the capacity of rangeland pastures to produce forage, in turn further complicating the means by which rangeland managers raise and graze livestock (Cook et al, 2015; Briske et al. 2021). For rangeland managers in the region, this means that previously successful management plans may not yield the same outcomes in future seasons (Joyce and Marshall, 2017). Thus, monitoring the response of these working ecosystems to specific management actions is now of utmost value to sustainable rangeland management.

1.1.2 Adaptive Rangeland Management

Much consideration has already been given to the subject of sustainable rangeland management in the SGS; indeed, the U.S. Department of Agriculture's Agricultural Research Service (USDA ARS) runs the Central Plains Experimental Range (CPER) in Nunn, Colorado, which has hosted many projects informing rangeland management in the region since 1939. The long history of research at the site allows for the evidence-based comparison of different rangeland management techniques and the long-term impacts those techniques have on this kind of landscape (Shoop et al. 1989; Lauenroth and Sala, 1992; Porensky et al. 2017). By utilizing this rangeland site, researchers at the USDA ARS generate much of the information useful to guiding sustainable livestock management in the SGS. They commonly find that, while there may not be one single best management option for all rangeland managers, there do exist a variety of management methods that are frequently successful (Derner et al. 2021). When informed by regular ecosystem monitoring, these management methods comprise a process called adaptive rangeland management (ARM), which can provide a framework for the sustainable grazing in the context of climatic extremes predicted to become more common to the SGS.

ARM is the approach in which land managers learn from the impacts of their past decisions to inform future best practices on the landscapes they manage. To utilize this approach, ARM requires a continuous cycle of assessment and decision making, including the following steps: the analysis of the dynamic landscape conditions, prioritization of management goals, implementation of a management plan, observation of management plan impacts, and back again to the analysis of landscape dynamics (Allen et al. 2017; Watson et al. 2019; Derner et al. 2021). With ARM, land managers can meet both the shifting needs of their given ecosystem as well as their production goals (Derner et al. 2022). This is not, as it may seem, a system based on simple

trial and error, but instead a structured approach of balancing control with uncertainty. Thus, a key difference in the ARM approach, especially in respect to this thesis, is that the system is constantly monitored to enable land managers to act in response to changing environmental conditions (Karl et al. 2017). However, this requires that land managers have access to quality, up-to-date data on the conditions of forage in their pastures. Direct observation of the entire landscape can be labor intensive and time consuming, but a variety of new technologies, such as remotely captured imagery, can condense this previously arduous task of landscape observation into a drone flight or satellite pass (Jansen et al. 2021; Browning et al. 202). With technologically advanced monitoring of vegetation conditions at the landscape level, ARM is a more accessible approach than ever before.

1.1.3 Factors Influencing Vegetation Conditions

In this spatially heterogenous landscape, ecosystem resilience, and therefore, ecosystem capacity to support livestock production, is highly dependent on variation in vegetation structure, composition, and diversity (Kelly et al. 2016). Cattle stocking rate, grazing intensity, timing of grazing, and pasture rotation are some of the ways rangeland managers can control this variation in vegetation, but other, less controllable factors affecting the plant community, such as shifts in seasonal temperature patterns or extended periods of drought, can also influence the resilience of the working ecosystem (Milchunas et al. 1988; Briske et al. 2021; Derner et al. 2021). New technologies, such as remotely sensed imagery, can allow rangeland managers a new method to quantify the impact of these factors on forage production in a continuous and rapid way that can be used to help in adaptively managing these landscapes (Rango et al. 2009; Browning et al. 2021; Wood et al. 2022). However, to utilize ARM in the SGS, and control for these conditions affecting vegetation, we must first understand the specific circumstances impacting these plant communities, and how these circumstances may be quantified by imagery. Phenological and physiological aspects of vegetation influence vegetation growth, and, consequently spectral imagery of vegetation across a landscape (Johnson et al. 2018; Wijesingha et al. 2020; Matongera et al. 2021).

The phenology of plant communities across the SGS controls the timing of vegetation growth and, thus, the timing of forages available for livestock and wildlife. Previous studies show that the phenological stage of vegetation can correlate not only to the magnitude of biomass accumulated in a pasture, but also to the relative nutritional value of forage plants at a

given time (Heitschmidt and Stuth, 1991; Rigge et al. 2013). In studies carried out in other North American rangeland ecosystems, some researchers utilize the timing of initial spring 'green-up,' 'peak greenness,' and autumn 'brown-down' to identify phenological stages at the landscape level, while others use more detailed, species-specific stages to understand plant development on the range (Denny et al. 2014). Satellite imagery, unmanned aerial vehicle (UAV) imagery, and pictures from mounted digital cameras have all been used to predict the relative phenological stage of vegetation using these 'greenness' benchmarks with varied success, but the shift of vegetation growth cycles predicted to result from climate change could further complicate this imagery application (Arzani et al. 2004; Johnson et al. 2018; Browning et al. 2019; Watson et al. 2019; Wijesingha et al. 2020).

The physiology of vegetation can similarly impact both the nutrition value of plants and the capacity of plants to accumulate biomass (Heitschmidt and Stuth, 1991). Healthy, growing vegetation is more nutritionally dense than distressed or dead forage vegetation. Both heat and drought can reduce the capacity of vegetation to photosynthesize and grow, in turn reducing chlorophyl activity and altering spectral reflectance of the vegetation as imaged by remote technologies. Studies analyzing the application of remote imagery in rangeland forage quantification commonly find that desirable, actively photosynthesizing leaf tissues yield significantly different leaf spectral reflectance values compared to the less valuable, mature, fibrous plant tissue (Johnson et al. 2018; Browning et al. 2019; Jansen et al. 2021). But, the ability of remote sensing technologies to accurately identify these physiological conditions, and moreover, the quality of forages, in droughted conditions in the SGS differs from pasture to pasture (Kearney et al. 2021; Irissari, 2022).

1.1.4 Imagery Applications

Previous studies demonstrate that different imagery technologies have varied applications in predicting phenological and physiological conditions of vegetation remotely, with caveats to each type of imagery. Satellite imagery, unmanned aerial vehicle (UAV) imagery, and land-based images can all help inform rangeland management practices, but each technology operates at vastly different scales and with different levels of temporal frequency. A land-based digital camera can capture photos spanning only the camera's limited field of view, which is, at most, a few square kilometers, but a land manager can capture these photos at any desired frequency (Browning et al. 2019; Watson et al. 2019; Browning et al. 2021). UAV imagery can span

multiple square kilometers, at a much higher level of detail, while capturing much more specific spectral information. The regularity of UAV flights throughout a growing season, is, however dependent on the availability of a UAV pilot and local weather conditions, as clear, calm conditions are required for imagery collection via UAV. (Wijesingha et al. 2020; Wood et al. 2022). Satellite imagery is slightly more robust to weather conditions, as atmospheric conditions will not prevent imagery capture; however, cloud cover, precipitation, and smoke from wildfires can create spectral noise that requires calculated spectral processing to overcome (Gómez-Chova et al. 2017; Moravec et al. 2021). Additionally, satellite passes are made on consistent, regulated schedules requiring only that land managers have access to relevant imagery, which spans thousands of square kilometers but cannot decern details seen by a land-based camera or UAV (Zhang et al. 2017). Any of these technologies can therefore be useful in ARM, but the choice of which technology to use is up to the individual land manager's needs.

Further, each of these technology options yield different types data, consequently giving land managers different capacities for analysis of landscape conditions. While digital camera photos can be compared throughout the season to visually contextualize landscape phenology and greenness, UAV and satellite imagery can be more deeply examined to help managers understand the vegetation in their rangelands (Browning et al. 2019; Johnson et al. 201). By comparing different bands of spectra, researchers have been able to use both satellite and UAV multispectral imagery to create vegetation indices (VIs) from which to evaluate vegetation conditions remotely (Wood et al. 2022). One of the most well studied VIs is the Normalized Difference Vegetation Index (NDVI). NDVI compares differences in reflectance of red and near-infrared wavelengths to define the spectral output of vegetative canopy across a landscape, thus quantifying the absorption of green spectra in chlorophyll pigments of leaves at a broad scale. This index simplifies this reflectance into a simple 'greenness' value, between -1 and 1. In this index, surfaces like dead plant cover or bare ground are defined as 0, plant canopies are defined between the values of 0 and 1, and open water is defined in values between 0 and -1. Further, plant canopies that are stressed or senescing correspond to lower values within this range while greener, vigorously photosynthesizing plant canopies correspond to higher values (Rouse et al. 1974; Zhang et al. 2017). Accordingly, NDVI can be an excellent tool in understanding vegetation phenology and physiology when the index is compared for the same landscape over the course of a season, as the capacity of vegetation to photosynthesize oscillates over the course

of a standard growing season (Pettorelli et al. 2005; Borowik et al. 2013; Robinson et al. 2017). Researchers working in rangeland ecosystems have used time-integrated NDVI to evaluate the spatial distribution of different grassland communities over time and detect phenological patterns with relative success (Matongera et al. 2021). However, the capacity of NDVI to correlate with vegetation condition does not always extend to forage quality. Previous work modeling landcover and phenology with NDVI in other rangeland systems have shown that measurements of forage quality are not well correlated to 'greenness' as measured by the index (Rigge et al. 2013; Browning et al. 2019). Specifically, NDVI has been shown to lose correlation to forage quality in late summer into fall, when vegetation is expected to begin to senesce or become drought-stressed. If cool-season precipitation allows plants to 'green up' again late in the growing season, vegetation can put on less nutritious, fibrous biomass, hence becoming lower quality livestock forage while simultaneously having similar NDVI values to the more nutritious spring forage. This 'false-positive' type of issue presented in NDVI by late season precipitation shows opportunity for a new vegetation model that might better capture vegetation conditions across wider climatic circumstances.

The consideration of additional spectral bands available in multispectral imagery could help make up for this loss of correlation between forage quality and VIs. Research utilizing other spectral bands, such as short-wave infrared (SWIR) bands, have been able to examine specific content of vegetation, like water, nitrogen, and protein (Hardisky et al. 1983; Johnson et al. 2018). Research into vegetation spectral reflectance has also explored the relationship of vegetation conditions to the angles that form between specific bands of reflectance. These kinds of indices, known as broadband spectral angle indices, or BAIs, can similarly be used to mitigate shortfalls of existing spectral indices by quantifying other details of vegetation condition, such as crop residue or fraction vegetation cover (Yue et al. 2020). Remote vegetation modeling that combines multiple condition indicators, such as VI's and BAI's, are thus able to predict previously-uncaptured conditions of vegetation, such as drought-stress or biomass accumulation (Knutson and Fuchs, 2016; Kearney et al. 2022). Biomass models of this kind tend to integrate multiple vegetation metrics, such as NDVI and BAI, through multispectral data capture, to predict the biomass accumulated at a given point in time, in a given landscape (Jansen et al. 2021; Kearney et al. 2021). More investigation is required to strengthen these applications for regular rangeland use, as the models established thus far largely remain accurate only when

utilized in the local ecosystems from which these models are heavily trained. Thus, the overall goal of my project is to help improve biomass estimates of rangeland vegetation using remotely-sensed products by evaluating a recently developed model on plots that vary in vegetation composition and canopy structure. To do this, I gathered satellite and UAV multispectral imagery, as well as on-the-ground vegetation metrics, for a single SGS site, over a single, drought-stressed growing season, to test the accuracy of NDVI and preexisting biomass models in predicting conditions of vegetation in a resource-limited rangeland system.

CHAPTER 2: INDICES AND MODELS IN NORTHERN COLORADO RANGELANDS

2.1 Introduction

An urgent issue threatening the global agricultural industry is the impact of climate change on our working ecosystems (Kukal and Irmak, 2017; IPCC, 2022). Rangelands are one kind of working ecosystem especially susceptible to alterations in global climate patterns, as the capacity of rangelands to support livestock is often dependent on seasonal precipitation (Havstad at al. 2007; Briske et al. 2021). In the shortgrass steppe (SGS), the warmest, driest portion of the Great Plains, the threat of extreme heat and drought only further complicate the challenges rangeland managers regularly face in balancing the needs of their cattle with the needs of their ecosystems (Havstad et al. 2009). The SGS is extraordinarily impacted by these extreme weather events such that vegetation can be severely impacted, causing shifts in phenological patterns, stunting growth, or even premature death of forage plants across entire pastures (Lauenroth and Burke, 2008). As such, the increasing likelihood of variable temperatures and frequent drought in grasslands like the SGS poses unique challenges to rangeland managers that rely on rangeland forage to support their livestock. The management of these systems in response to these variable weather patterns is fundamental both to help sustain the health of these ecosystems and the economic strength of our agricultural systems (Jones et al. 2021).

Adaptive Rangeland Management (ARM) is one approach to manage these ecosystems that could help mitigate the negative impacts of novel climate patterns on forage production (Derner and Augustine, 2016; Allen et al. 2017). ARM requires that rangeland managers be able to constantly monitor their landscapes for changes in vegetation condition so they can continually adjust their management actions (e.g., grazing location, grazing intensity, etc.) to meet their economic and ecological goals (Derner et al. 2022). Although recognized as an ideal strategy, the labor involved in continuously monitoring the vegetation across a working landscape can become prohibitive to the regular implementation of ARM. However, new remote imaging technologies, such as multispectral imagery, could help rangeland managers monitor the condition of vegetation in their pastures on a regular basis by passive means.

Remotely sensed products are currently available to provide information on rangeland vegetation (http://rangelands.app), but the accuracy of these tools varies by ecosystem type,

vegetation condition, and spatial scale of interest (Fuhlendorf et al. 2017; Bielski et al. 2021). Models can be built from available satellite imagery for specific sites to predict biomass available for forage for rangelands experiencing a variety of environmental conditions, vegetation types, or grazing patterns, but these models have not been widely tested (Kearney et al. 2022; Roberts et al. 2022). For one such model, Kearney et al. (2022) used multispectral imagery to monitor and estimate biomass production on SGS rangelands in an area with native SGS vegetation. By combining site-specific indices from multiple spectral bands, the authors were able to explain 75-79% of the biomass variation in their model. The success of their model, and the varied success of the other models tested in this study, validate the combined use of spectral indicators for biomass modeling, and shows the promise of biomass modeling as a tool in adaptive rangeland management. However, biomass models such as this are not yet widely used and have yet to be tested across a wide variety of rangeland ecosystems, especially in ecosystems different from where the model was trained.

This research investigates the ability to transfer, retrain, or refit existing remote sensing models of forage biomass, for use in informing ARM. Although plant communities in the SGS region are generally drought-adapted, short-statured, and grass-dominated, it is yet unclear how sensitive these vegetation indices and models can be to the range of plant communities found in the SGS. To address these gaps in understanding, I groundtruthed vegetation indices built from two different sources of remotely-captured imagery with on-the-ground forage conditions across co-located pastures with different canopy structures and species compositions through a single growing season. To test the capacity of biomass models under droughted conditions, I tested an existing biomass model recently built at a nearby SGS site in addition to training and testing four other potential biomass models. I hypothesized that existing models built for the SGS would be challenged by the extreme conditions, but that those models may offer a good starting point from which to train similar models at my specific site.

2.2 Methods

2.2.1 Study Area

This study was conducted at Colorado State University's Gabbard-Rutledge Property, 300 acres of naturalized shortgrass rangeland outside of Waverly, CO (~ 40° 42' N, 105° 06' W; Figure 2). The topography of the property is relatively flat, with slopes between 1 and 10%, and

elevation from 1580 meters to 1596 meters above sea level (USDA, 2013). Lower areas in the site contain ephemeral wetlands that extend from the southeast corner of the property northwest into the center, but these areas were not utilized in this study. The property is organized into multiple pastures around the center wetland, fenced decades prior to this project, according to both utility and biological composition. In order to assess the impact of different SGS plant community compositions on NDVI (the Normalized Difference Vegetation Index) and plant biomass models, I utilized two different pastures. The first of the selected pastures was the westernmost pasture, which represented a homogenous vegetation canopy and was dominated by *Psathyrostachys junceaus (*Russian Wildrye), a species commonly planted on CRP land as a forage grass for cattle. The second or easternmost pasture, represented a more heterogenous shortgrass composition and was comprised largely of the perennial C3 grass *Agropyron cristatum* (Crested Wheatgreass) and the native shrub *Chysothamnus viscindiflorus* (Yellow Rabbitbrush). Crested Wheatgrass is another species commonly planted as a forage grass and rabbitbrush is an early successionally species that colonizes sites after disturbance, which is also commonly found on CRP land. Hereafter these two pastures are referred to as the wildrye or wheatgrass pastures. The soils encountered at the site were deep, well drained loams; Kim Loam in the westernmost pasture and Stoneham Loam in the easternmost pasture (USDA-NRCS, 2013).

2.2.2 Summer Precipitation

All study measurements were carried out during the spring and summer of 2022. This growing season was relatively dry and the amount of spring precipitation was lower than the historical average (Figure 1). To further evaluate the sites precipitation, I used historic and recent precipitation data from a weather station ~3 miles from the site. This region is known for spatially heterogeneity in weather events (Augustine, 2010), and some of the precipitation events shown in Figure 1 did not occur at my field site. Specifically, the precipitation events in May and July seen in Figure 1 did not occur at the Gabbard-Rutledge site (personal observation), and so conditions at my site were likely much drier than what is represented.

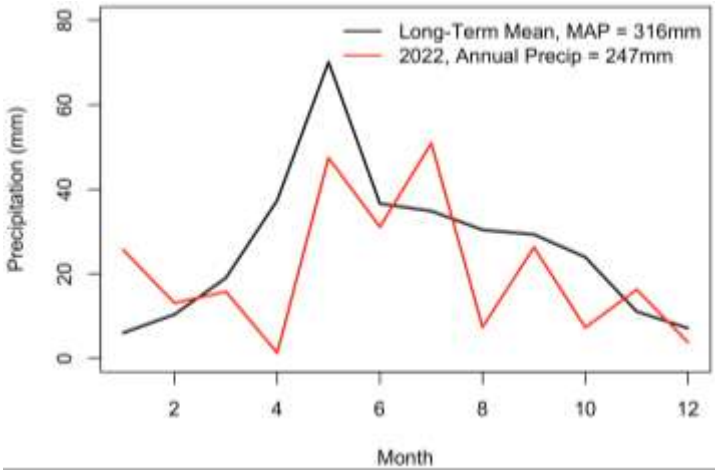

Figure 1: Precipitation for the Gabbard-Rutledge research site. Data was retrieved from the Global Historic Climate Network using the National Centers for Environmental Information, of the nearest available weather station (Station ID: US1COLR0140). The long-term averages, derived from data ranging 2000-2022, and are shown in black. The monthly precipitation for 2022 is shown in red.

2.2.3 Species of Study

The forage species I measured in this study were the dominant species in each pasture. The species I encountered in the pastures and their approximate cover can be found in *Table 1*. In the western pasture, the dominant plant species was *Psathyrostachys junceaus* (Fisch.) or Russian Wildrye, with scattered patches of *Bromus inermis* (Leyss), or Smooth Brome, and a few individuals of *Chysothamnus viscidiflorus* (Hook.), or Yellow Rabbitbrush, spread across the entire pasture. I termed this pasture the Wildrye pasture for this project. As such, I measured only the wildrye in this pasture and disregarded all other species. In the eastern pasture, the dominant species were *Agropyron cristatum* (L. Gaertn.) or Crested Wheatgrass and *C. viscindiflorus*, with various forbs and patches of *B. inermis*. I termed this pasture the Wheatgrass pasture; I measured only wheatgrass in this pasture and disregarded all other species.

Table 1: Biological information on species frequently encountered in this study. Visual estimations of plant coverage are also included, represented as percentages of pasture surface. Estimations were made in May of 2022, before any changes to composition were enacted in either pasture.

Species	Plant Functional Group	Forage Use	% Cover Wildrye Pasture	% Cover Wheatgrass Pasture
Chrysothamnus viscidiflorus	shrub	fall to winter	5%	25%
Agropyron cristatum	bunchgrass	Spring	0%	50%
Psathyrostachys junceaus	bunchgrass	summer to fall	65%	0%
Bromus inermis	rhizomatous grass	spring and fall	13%	8%

2.2.4 Experimental Design

In each of the two pastures I established three blocks based on consistency in visual estimates of biological composition, but the blocks helped control for variation in soil texture and topography. Within each of the six blocks (2 pastures X 3 blocks/pasture) I established a control plot and the pasture-relevant treatment plots as shown in Figure 2. Each plot

Figure 2: Map of Gabbard-Rutledge Property inset with site locator map. Research plots utilized in this study are outlined in black, with fill patterns to indicate treatments. Geolocated ground control points surrounding the plots are marked in orange. For the uses of this study, the eastern pasture, which encompasses seven plots, is known as the 'Wildrye' pasture, while the western pasture, which encompasses thirteen plots, is known as the 'Wheatgrass' pasture.

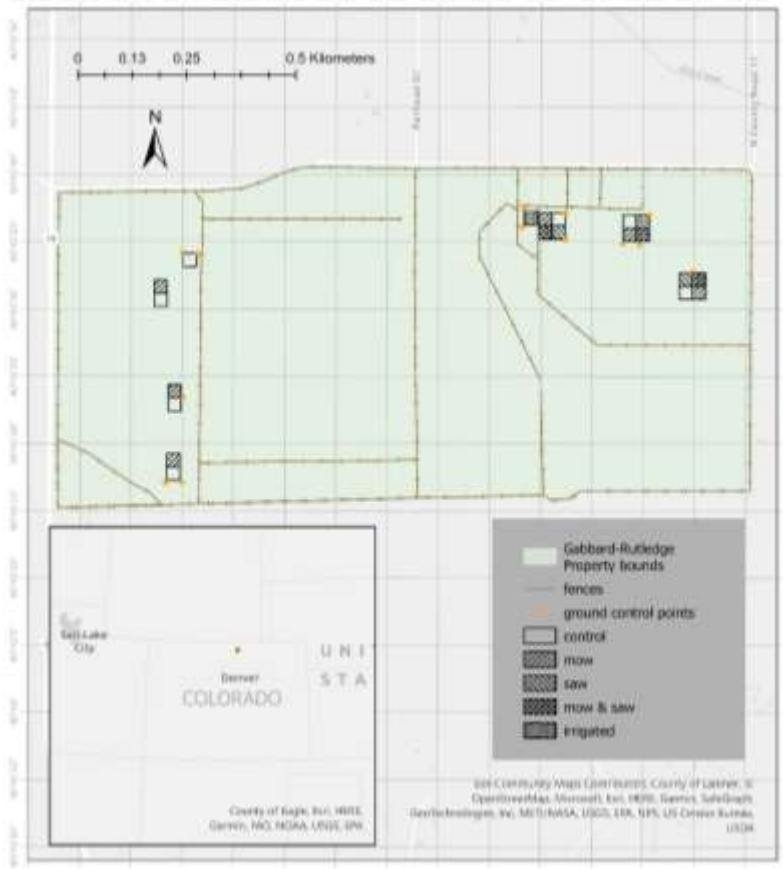

encompassed 30 x 30 m of pasture, with the outer 5 m on each side utilized as a 'buffer'. This buffer allowed me to collect the necessary spectral data from each plot inset with minimal influence from outside imagery. Thus, I made ground-based measurements in only the inner 20 x 20 m plot. Additionally, from each plot I randomly selected four individuals of the treatment-relevant forage species from diagonally placed transects running between two opposing corners from which to collect measurements on the ground for imagery comparison. Consequently, through the course of this project I monitored a total of 20 unique plots that included 80 individual plants.

To examine the effect of compositional and structural differences in remotely-estimated forage, I manipulated the plots in three ways. First, I removed the previous year's dead in some plots in both pastures by mowing the dead biomass left standing above the new season's growth. This changed the vegetation structure as well as the proportion of brown to green biomass. Given that this research is intended for rangeland use, I additionally considered the treatment of mowing a proxy for grazing in the system, to simulate the canopy change of cattle consumption and the imagery captured thereof. In the wheatgrass pasture, I changed the vegetation composition and structure through the removal of the woody shrub *C. viscidiflorus* from the

assigned plots. I assigned these treatments to the plots within each block randomly, and implemented each treatment to the full 30 x 30 m plot. Since there were no shrubs on the wildrye pasture, the only biomass removal that occurred was that of mechanical mowing. This resulted in each of the three wildrye blocks containing two plots, a control, and a mowed plot. The treatments I enacted in the wheatgrass pasture were those of biomass removal, via both mechanical mowing and shrub removal, together and independently, which resulted in 4 plots per block on this pasture: control, mowing, shrub removal, and both mowing and shrub removal together. Additionally, in the wheatgrass pasture, I also included an extra treatment plot in just one of the blocks as a stand-alone irrigation treatment.

I enacted the mowing treatment mid-season, from the last week of June through the first week of July. To do this, I operated a Billy Goat Outback 24-Inch 13HP Honda Rough Cut Brush Mower (BC2403H, Briggs and Stratton, Milwaukee, WI), with the blade set at a height of approximately 12 cm, to mow the entirety of the selected plots. Once mowed, I manually raked each plot to remove the cut biomass. I discarded all cut biomass a minimum of 5 meters outside the 30 x 30 m plots, with the goal of minimizing the spectral influence of cut biomass on the largest imagery pixels.

I carried out the shrub-removal treatment earlier, from mid- to late May. I used a DeWalt Flexvolt 60V 16in Chainsaw (UPC 885911636322, DeWalt Industrial Tool Co., Towson, MD) to cut every *C. viscidiflorus* individual growing in the randomly assigned shrub-removal treatment plots. I cut each to a maximum stump height of 12 cm, both to minimize the potential impact of stumps in the imagery, and to allow clearance for the mowing equipment in the plots that were both sawed and mowed. Again, I discarded the cut *C. viscidiflorus* a minimum of 5 meters outside the 30 x 30 m plots to minimize the influence of cut shrubs on the largest imagery pixels.

As the season progressed without notable precipitation, I added an irrigation treatment to the stand-alone plot in the wheatgrass pasture. I intended for the irrigation treatment to simulate an additional 1.5 inches of rain, spread over two rain events. To accomplish this, I built an irrigation system composed of a 100ft diameter coverage Strongway tripod sprinkler (49506, Northern Tool and Equipment, Burnsville, MN), a 12V SHURflo diaphragm pump (2088343500, Pentair PLC, Golden Valley, MN), a GPI turbine type flow meter (GPImeters, Sparta, NJ), and 150 meters of standard ¾ inch garden hose. I utilized the main water spigot on the property to supply the system and ran the pump 3 meters from the spigot to maintain

adequate water pressure for the desired sprinkler coverage. I alternated the sprinkler's position between the southeast corner and the northwest corner, setting the spray range to 90° of spread to cover the plot from the two opposing corners. I ran the irrigation system twice, for two separate sessions lasting approximately 11.5 hours each, on July 30 and August 7. In that time, the plot received a reported 9000 gallons of water. This treatment was not replicated in the study and so I cannot make statistical inferences about this treatment compared to others.

2.2.5 Ground-based Measurements

Throughout the course of the 2022 growing season, I utilized a variety of ground-based methods to quantify the vegetation and serve as ground-truthing metrics from which to test unmanned aerial vehicle (UAV) and satellite multispectral imagery. The measurements I made included plant phenophase, stretched plant height, observed greenness, and end-of-season biomass.

For consistency of phenophase, stretched height, and observed greenness measurements, I randomly selected four individuals of the treatment-relevant forage species from a transect running from inset to exterior of each plot. Thus, my dataset for these repeated measurements was built from 28 *P. junceaus* individuals, from the wildrye pasture, and 52 *A. cristatum* individuals, from the wheatgrass pasture. I visited these individuals 6 times between May and September 2022. To quantify growth and development, I surveyed phenological stage and stretched height of each individual plant selected. I characterized individual plant phenology with the standardized phenophases outlined for use by the National Ecological Observatory Network (Denny et al. 2014). The phenophases, or phenological stages, differ for each plant functional group, and each stage is based on the start- or end-point of specific observable stages in annual life cycles. Because I focused my measurements on forage species, I utilized only the grass phenophase categories described in Table 2. To measure stretched height, I recorded the height of each plant from base to tallest point on a meter stick while gently stretching the plant to its full upright height. Then, I recorded my own observations of greenness for each plant, as a percentage of the whole individual.

Table 2: Standardized grass phenophases as described by Denny et al. (2014).

Phenophases	Description	Phenophase Quantifier
Vegetative Phenophase	Initial growth	What percentage of the plant is green?
Reproductive Phenophase	Flowers or flower buds	How many fresh flower heads are present?
	Pollen release	How much pollen is released?
Fruit/Seed Phenophase	Fruits	How many fruits are present?
	Ripe fruits	What percentage of all fruits (unripe plus ripe) on the plant are ripe?
	Ripe fruit/seed drop	How many mature fruits have dropped seeds/ been removed since your last visit?

To estimate biomass in each plot, I clipped and bagged all herbaceous biomass from a randomly placed 0.1 m^2 quadrat in the buffer zones of each plot during my last site visit in September. I made these collections on each side of the buffer zone, such that I had four samples for each plot. I oven-dried the bagged samples at 50°C for 72 hours before sorting each collection by both leaf and stem as well as color (Weiss et al. 2020). I weighed each component for an estimate of total and green biomass and for leaf to stem ratio. These biomass totals then represented the 'truth' from which to test the imagery derived biomass models. To analyze the results of my ground-based observations, I employed two-ANOVAs, as well as treatment and pasture means where applicable, which I compared visually as boxplots. I utilized an $\alpha < 0.05$ to detect statistical significance in my findings.

2.2.6 Imagery Collection

The two types of imagery evaluated in this project were local UAV-collected multispectral imagery and Sentinel satellite multispectral imagery. Imagery was collected and compared across five flight dates during the summer of 2022. To acquire local UAV-collected imagery of the study pastures, I coordinated with an experienced UAV pilot, operating a DJI Matrice 210 V2 quadcopter (SZ DJI Technology Co., Ltd., Shenzhen, China), equipped with a 10-bandmultispectral camera (Model# 805-00057, MicaSense, Inc., Seattle, WA). Together, we installed ground control points just outside of plot perimeters to optimize spatial accuracy in image processing (Figure 2). The UAV-pilot and I utilized an Emlid Reach RS+ GPS Coordinate System (1092, Budapest, Hungary) to geolocate each ground control point in order to align the collected imagery. Using preprogrammed flight paths, the UAV pilot conducted five flights throughout the season; four flights spanning both pastures and one flight over only the wildrye pasture. Each flight took place in early afternoon, with clear and calm local conditions. Flights were set to an altitude of 90 meters, yielding a pixel size of 6.7 cm for the collected imagery.

With the set speed of 5 meters per second, and a forward and side image overlap of 80%, the flightpath over the combined pasture extents took around 18 minutes to complete. We then utilized Agisoft Metashape (version 1.7.2; agisoft.com; Agisoft LLC, St. Petersburg, Russia) to process these flight images into geographically aligned, atmospherically corrected, orthomosiacs. To acquire Sentinel imagery of the study pastures, I downloaded Sentinel 2A MSI 1C imagery of tile 13TDF from the Copernicus Open Access Hub (https://scihub.copernicus.eu/) for the matching dates of interest. I selected imagery from satellite passes that were (a.) within two days of UAV collection, and (b.) clear of atmospheric interference. I also ran each of the selected Sentinel images through ESA's Sen2Core Processor (Main-knorn et al. 2017) to further minimize atmospheric interference, yielding 2A MSI 2A images (Moravec et al. 2021).

Once I had collected all imagery relevant to this project and processed each for alignment and atmospheric noise in their appropriate applications, I imported the imagery into ArcGIS Pro (version 3.1.1; esri.com; Esri Inc. Redlands, CA) and applied the 'Rescale' Data Management Tool to interpret each of the differently scaled spectral data into 10 m pixels using the nearest-neighbor resampling option. I then clipped each image to the bounds of each of the 20 x 20 m plots via the Clip Raster tool, and calculated the mean spectral values of pixels encompassed in each plot. These averaged values represent the reflectance utilized for each band, for each passing date, to build vegetation indices and models for each plot that could be compared between Sentinel and Micasense products.

2.2.7. Vegetation Indices and Statistical Models

With the imagery processed, rescaled, and clipped, I utilized specific spectral bands to create vegetation indices as well as biomass models similar to previous research (Wijesingha et al. 2020; Kearney et al. 2022). The range of wavelengths of each spectral band differed slightly between Sentinel and the UAV-collected imagery, with information on these specific bands in the Appendix (Supplemental Table 1).

To derive NDVI from the processed Micasense orthomosiacs, I recombined the three bands of interest from each plot inset for the final flight date, using the 'Band Arithmetic' tool in ArcGIS Pro. See Supplemental Table 1 for a list of Micasense and Sentinel spectral bands used in this study. The bands utilized from the Micasense collections for this were RED1 (642-658 nm), RED2 (663-673 nm), and NIR (820-860 nm). I added together the reflectance of both available red spectral bands in an effort to capture the spectral range contained within the

broader red band available in the Sentinel 2A imagery (649-680 nm). The NIR bands from the Sentinel (855-875 nm) also differed slightly compared to the Micasense. After exporting the index as a raster for each plot inset, I imported the rasters into R Studio and averaged each inset index value within each pasture, by both plot and treatment. The NDVI differences across treatments proved insignificant ($p > 0.05$), so for further analysis, I utilized the mean of the plot index values for each pasture.

To derive NDVI from the processed Sentinel satellite imagery, I recombined just two bands of interest from the final passing date of interest, again using the Band Arithmetic tool in ArcGIS Pro (version 3.1.1; esri.com; Esri Inc. Redlands, CA). These bands were RED (649-680 nm) and NIR (855-875 nm). I then exported this index from ArcGIS Pro, in addition to the spectral bands required to build biomass models. The other spectral bands of interest from Sentinel were GREEN (542-577 nm), and SWIR2 (2215-2290 nm). In RStudio, I averaged each index and band values within each pasture, by both plot and treatment, as, again, treatments within each pasture were not significantly different from each other ($p > .05$) (RStudio Team, 2023).

To fit model parameters and compare model predictions to observed values, I used RStudio (R Core Team, 2023). I began the construction of statistical models to explain biomass utilizing the available spectral bands from the last date of imagery collections, Table 3 shows the variables included in each model. I used the HLS-only model equation from Kearney et al. (2022) as a starting point from which I made different variations that might correlate to on-the-ground biomass. For some model variations, I used fewer variables than the Kearney model in order to test whether all the variables are required to explain the variability in forage biomass observed at my study site. I also included some models with NDVI, in addition to NDII7 as the original model utilized, to investigate the influence of the RED bands in addition to NIR and SWIR2 in vegetation modeling (Rouse et al. 1974; Ji et al. 2011; Johnson et al. 2018).

Table 3: Biomass model equations as well as input features to tested biomass models, as created from Kearney et al. (2022).

Feature	Description	Formula
Biomass Models		
Kearney HLS-only (Kearney et al. 2022)	Kearney HLS-only Biomass Model utilizing features available from the Harmonized Landsat-Sentinel (HLS) dataset	*NDII7 + BAI_236 + NIR*
Behnke A (Kearney et al. 2022)	Kearney HSL-only Biomass Model utilizing features from Sentinel 2A MSI2A	*NDII7 + BAI_236 + NIR*
Behnke B (Kearney et al. 2022)	Edits to Kearney HLS-only Biomass Model utilizing features from Sentinel 2A MSI2A	*NDII7 + NDVI + BAI_236 + NIR*
Behnke C (Kearney et al. 2022)	Edits to Kearney HLS-only Biomass Model utilizing features from Sentinel 2A MSI2A	*NDII7 + NDVI + BAI_236*
Behnke D (Kearney et al. 2022)	Edits to Kearney HLS-only Biomass Model utilizing features from Micasense orthomosiacs	*NDVI + NIR*
Vegetation Indices (VI's)		
NDVI (Rouse et al. 1974)	Normalize Difference Vegetation Index	$\frac{(NIR - RED)}{(NIR + RED)}$
NDII7 (Ji et al. 2011)	Normalized Difference Infrared Index 7	$\frac{(NIR - SWIR2)}{(NIR + SWIR2)}$
Broadband Angle Index		
BAI_236 (Yue et al. 2021)	BAI (GREEN, RED, SWIR2)	$180 - tan^{-1} \frac{reflectance(RED-GREEN)}{midpoint(RED-GREEN)/2500} + tan^{-1} \frac{reflectance(SWIR2-RED)}{midpoint(SWIR2-RED)/2500}$
Singular Band		
NIR	Sentinel Band 8A or Micasense Band 10	Near-infrared spectral range (0.85–0.88 μm)

To train and test new biomass models, I first subset the relevant data for each of my 20 unique plots into two groups of 10 plots via random assignment. I utilized one subset to estimate the parameter values for the model (i.e. model training) and used the other subset to test the accuracy of each model in predicting standing plant biomass. The first model I developed (model A) used the same parameters as the Kearney model, but I developed new coefficient values for each parameter for my specific study site. The other two models I developed (models B and C)

were selected to compare the use of RED bands in predicting biomass, in addition to and instead of the standalone NIR band. I built model D to utilize the comparable bands available from the Micasense imagery, since it was limited in variables without the SWIR2 band.

To train each model variant, I used linear regression, with mean biomass as the response variable and the selected variables as independent variables. I then used the output model coefficients to create the equations in which to input the spectral variable values from each of the 10 plots in the second subset, to generate predictions of standing biomass in each plot. I completed this process for both total and green biomass collections. The coefficients I utilized in each model equation are shown in Supplemental Table 2 and Supplemental Table 3.

2.3 Results

2.3.1 Ground-based Measurements

The ground-based measurements of phenology, visual greenness, stretched height, and biomass provided information on the conditions of forage in the two pastures I studied, with the treatments of mowing, shrub-removal, and irrigation providing variation within those forage conditions. Phenologically, I observed few significant differences across blocks, treatments, pastures, or time, as very little development occurred in the individuals I measured. I found that 60 of the 80 individuals I measured remained in the first vegetative phenophase for the entire growing season. This was most evident in the wildrye pasture, as none of the 28 *P. junceaus* progressed into reproductive maturity. The wheatgrass pasture, however, did yield some reproductively mature individuals, with 16 of 52 *A. cristatum* individuals producing fruits by the end of the season. There were no statistically significant differences in phenology of monitored wheatgrass individuals within or across treatments.

I found statistically significant differences in greenness between the two pastures and across time during 2022 (Figure 3). In both pastures the greenness was significantly different over time ($p < 0.001$), but not between treatments. Approximately 90% of the monitored individuals in the wildrye pasture were >50% brown by mid-July, with 11 of the 28 *P. junceaus* plants becoming completely senesced by mid-September. Over half of *A. cristatum* individuals were >50% green by mid-July, with only 6 of the 52 plants becoming completely brown by mid-September. Further, individuals in the single irrigated wheatgrass plot were greener than all other

plots on my final visit in September (Julian date 257), but at no other point in the season was this the case. I did not establish replicates for this treatment, so this difference cannot be considered significant.

Figure 3: Greenness for each treatment over time, represented as boxplots. The top panel contains the greenness measured in the wheatgrass plots; the bottom panel contains greenness measured in the wildrye plots. Treatment events of mowing (green dashed line) and irrigation (blue dotted line) are indicated by vertical lines. Treatments are indicated by color.

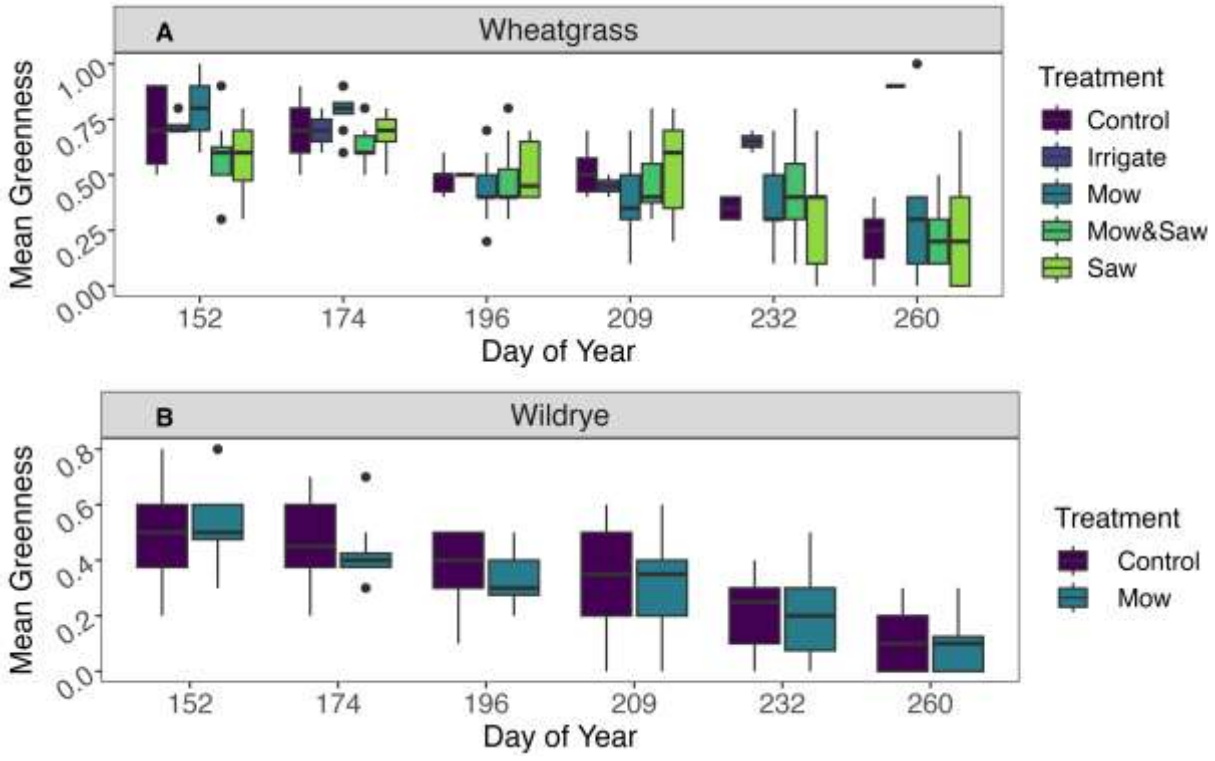

The results of the stretched plant height measurements similarly reflect the limited plant growth that occurred during the measurement period (Supplemental Figure 2) but, again, with significant differences between the two pastures studied. In the wildrye pasture, I found that stretched plant height was not significantly different across time or treatment. The mean stretched height of all 28 selected wildrye individuals in the wildrye pasture was 14.18 cm ± 1.29 (SE) in the beginning of June, and increased to 15.25 cm ± 1.48 (SE) by mid-July and 15.5 cm ± 1.88 (SE) by mid-September. Similarly, in the wheatgrass pasture, I found that stretched plant height was not significantly different across time or treatment, with the single exception of the irrigated plot on the final measurement date in September. In the wheatgrass pasture, the mean stretched height of the 52 individuals was 19.62 cm ± 2.43 (SE) at the beginning of June, which increased to 20.54 cm ± 2.07 (SE) by mid-July, and further, to a pasture mean of 22.55 cm ±

2.32 (SE) by mid-September. The variance in stretched height was smaller in the biomass removal plots, but this was due to the fact it was mowed, bringing all individuals to a similar height. The wheatgrass in the single irrigated plot reached a significantly taller mean stretched height of 29.53 ± 0.29 (SE) for the final mid-September measurement. This plot mean was significant in comparison to all other treatments ($p < 0.001$), on all other visits, but is made up of a much smaller sample size (n=4) as I was unable to replicate this treatment.

When comparing total standing biomass measured at the end of the growing season (Figure 4A) in September I found significant differences between blocks ($p= 0.008$) and treatments ($p < 0.001$), but not between the two pastures. However, when comparing only the green biomass (Figure 4B), which I assumed to be current year's growth, I observed differences across blocks ($p < 0.001$), treatments ($p < 0.001$), and pastures ($p < 0.001$). Further, the current years biomass clipped from plots in the wildrye pasture was significantly smaller than that clipped from any treatments of the wheatgrass plots. Within the wheatgrass plots, I found that the irrigated plot yielded current year biomasses significantly larger than the mean of most other wheatgrass treatments (mowed, shrub-removal, and mowed and shrub removal) as well as the wildrye treatments (control and mow). As such, the irrigation treatment was the source of treatment effects within the dry

Figure 4: Dry weight of all clipped foliage from collections made at end-of-season (mid-September). The panels on the left show biomass from wheatgrass plots wildrye plots are shown on the right.

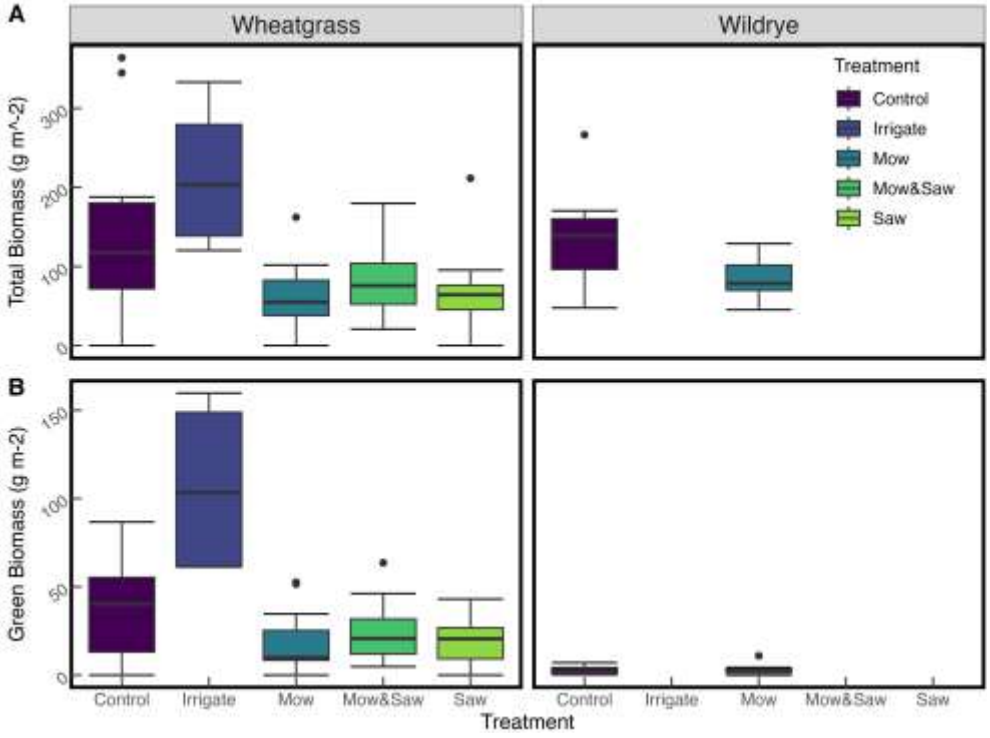

weights of green foliage. No other treatments yielded significant differences in biomass accumulation.

2.3.2 Comparing Vegetation Indices

NDVI generated from the two remotely-captured imagery sources (Sentinel Satellite vs. UAV-mounted MicaSense) differed from each other under most conditions (Figure 5). However, when comparing NDVI values from a single source across treatments, only the irrigated plot differed in the NDVI value ($\alpha < 0.05$), but this difference was only present in the final, mid-September imagery collection, and only from the local UAV flight. When comparing the indices, I averaged the NDVI values of each source to the pasture level, excluding the irrigation treatment, for each point in the 2022 season. The general trend in NDVI from the two sources across the season was similar, but the Micasense imagery always resulted in higher NDVI values and had higher variability among plots within each pasture (purple vs. blue lines in Figure 5A).

When compared in a linear regression model, the slope and intercept suggest important differences between these sources (Figure 5B). NDVI values from the Sentinel were always lower and less sensitive than the Micasense, resulting in a slope < 1 (0.423) and intercept > 0 (0.034). Further, although the two metrics are significantly correlated (p

Figure 5: NDVI timeseries derived from both UAV (Micasense) and satellite (Sentinel) imagery sources. Symbols represent the mean NDVI values of each pasture for each imagery source, as treatments were insignificant within each pasture. Error bars represent the standard error for the NDVI values.

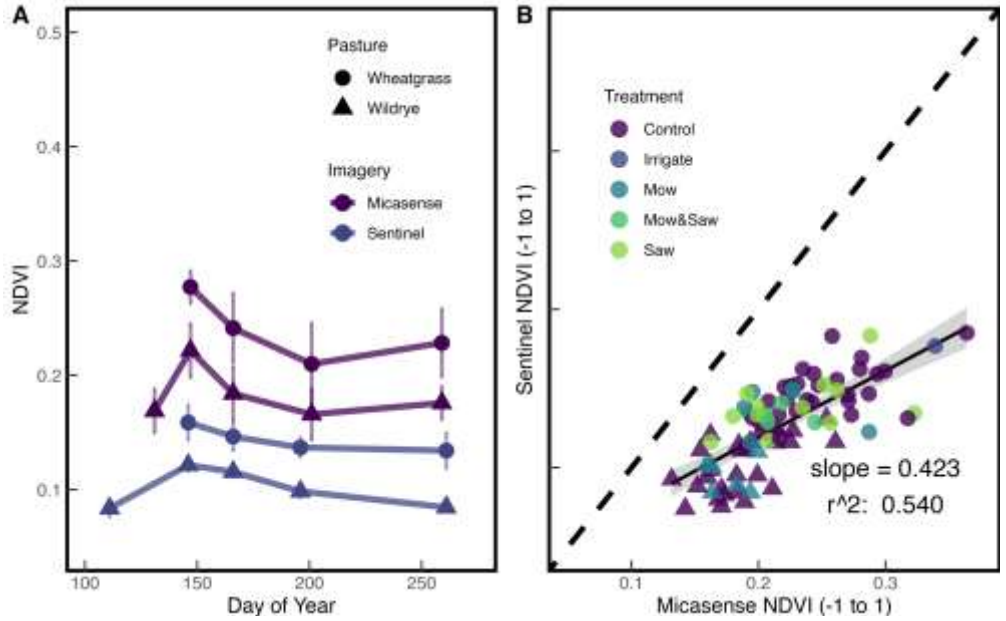

< 0.001), the Micasense-derived index only explains 54% of the variation present in the Sentinel-derived index (Figure 5B).

Figure 6. Correlations between ground-based measurements of canopy greenness and plant height Vs. NDVI

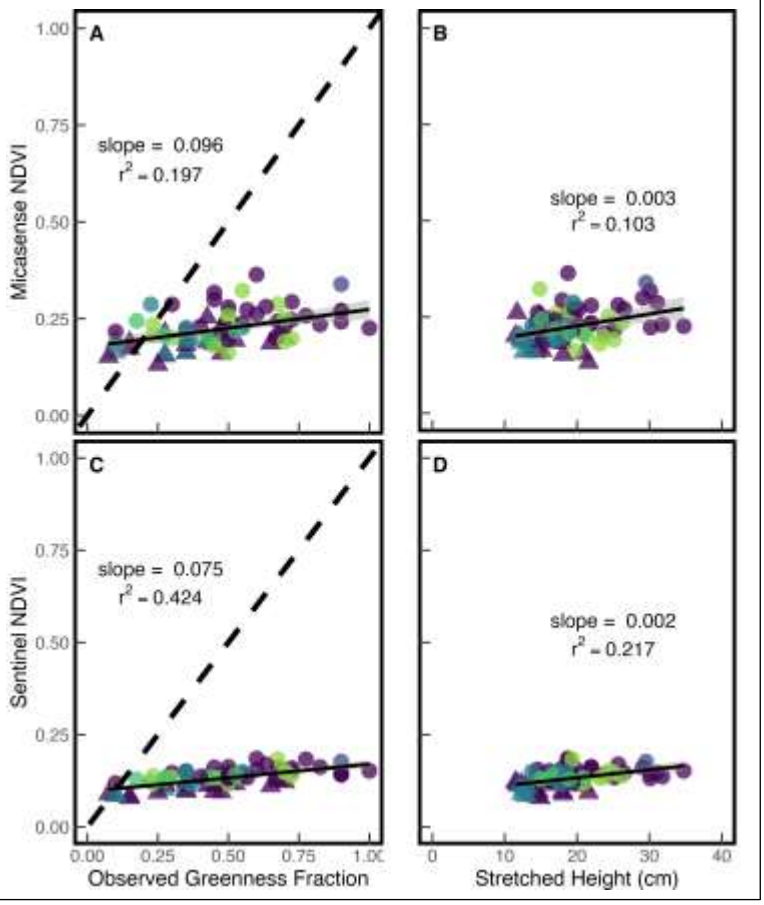

To analyze the sensitivity of these two imagery sources to pasture conditions, I compared the NDVI value of each plot to the ground-based measurements of pasture conditions measured throughout the season. Since both canopy greenness and stretched height exhibited differences between pastures and/or over time I compared these metrics to NDVI, and both variables yielded statistically significant relationships with NDVI calculated for both the Sentinel and Micasense.

For observations of visual greenness, I found that linear regressions between NDVI and greenness had slopes < 0.1 (Figure 6A and 6C). Both NDVI metrics showed very low sensitivity to changes in greenness, but the regressions were both significant ($p < 0.001$). There was less variation in the relationship for the Sentinel-derived NDVI ($r^2 = 0.424$) than the Micasense ($r^2 = 0.197$). The linear regression models comparing each of the two indices with measurements of stretched height (Figure 6B and 6D) responded similarly to those of visual greenness, in that the Sentinel-derived NDVI captures more variation in ground measurements of stretched height than the Micasense-derived NDVI when imaging the same pasture. Indeed, the Micasense-derived index captures only 10.3% of the observed variation in stretched grass height (Figure 6B) while the Sentinel-derived index accounts for 21.7% (Figure 6D). However, unlike the models utilizing greenness, the regression model for the Micasense-derived index yields a slightly shallower slope.

Like greenness and plant height, there was a significant correlation between current year biomass and NDVI from both sources, as shown in Figure 7. There are fewer data points in these regressions because only end-of-season measurements were utilized for biomass where greenness and plant height were collected bi-weekly throughout the season. However, the correlation between total standing biomass and NDVI was weak for both sources (Figure 7A and 7C), with only 16.5% (Micasense-derived NDVI, Figure 7A) and 4.8% (Sentinel-derived NDVI, Figure 7B) of the variability in the NDVI metrics explained by ground-based measurements. When only current-year biomass (i.e. 'Green Standing Biomass') was used, the correlation between ground-based measurements and NDVI metrics improved, with ~61% and ~69% of the variability in Micasense-derived NDVI (Figure 7B) and Sentinel-derived NDVI (Figure 7D) explained, respectively.

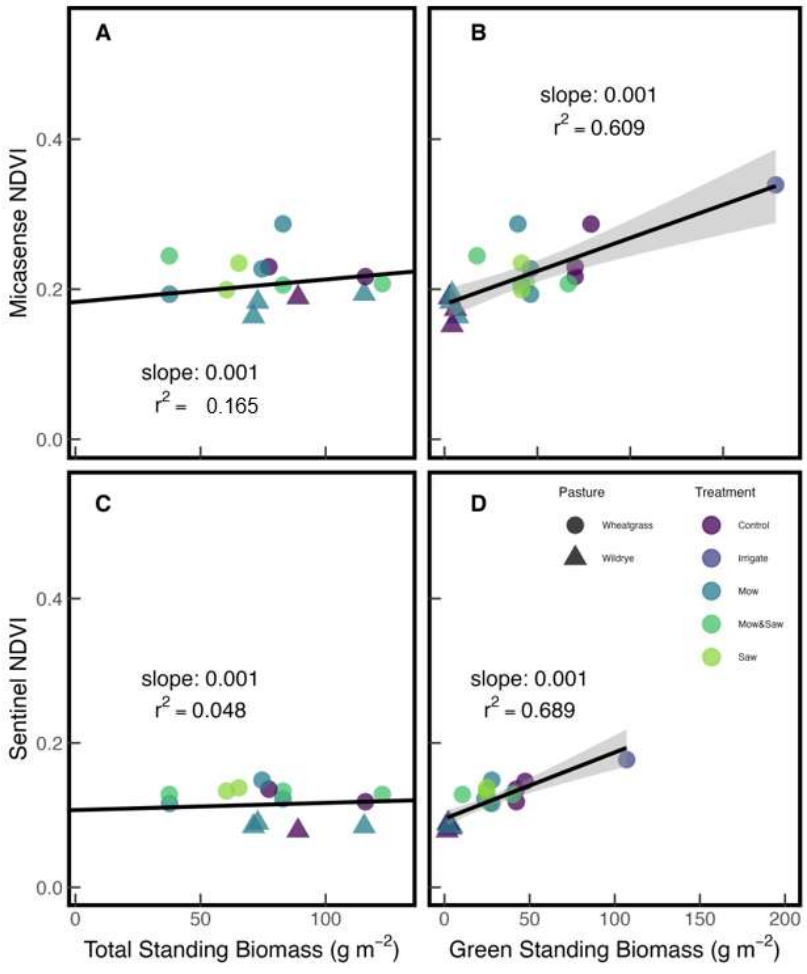

Figure 7: Linear regressions of total and green standing biomass clipped at the end of the growing season. NDVI values derived from drone-mounted imagery are on the top row (panels A&B) and NDVI from the Sentinel are on the bottom row (panels C&D). Total standing biomass (g m-2) are on the left column (panels A & C) while green standing biomass (g m-2) are on the right (panels B & D). Symbols represent the mean of each treatment in each pasture on the last sampling period of the growing season (September 16-18).

2.3.3 Biomass Models

I found that the biomass model developed by Kearney et al. (2022; hereafter referred to as the 'Kearney' model) for the shortgrass steppe was better at predicting green, current year

standing biomass than total standing biomass (Table 9), which included dead standing material produced during the previous growing season (Figure 8, triangles). When used to predict total standing biomass, this model accounted for only 5.6% of variation observed in the mean biomass clipped from each plot (Figure 8A), and the slope was not statistically significant at the $p < 0.05$ level. However, when employed to predict only the green biomass standing in those same plots, the Kearney model did have a significant slope ($p = 0.05$) and accounted for 64.4% of the variation (Figure 8B).

Table 9: Responses of biomass model predictions when regressed against mean clipped above-ground biomass. Models A-C were built from the September 18 Sentinel orbital pass, Model D was built from the September 16 local Micasense imagery collection. Significant p-values, at the $p < 0.05$ level, shown in bold.

Total Standing Biomass										
Model	**Kearney Model**		**Model A**		**Model B**		**Model C**		**Model D**	
R-squared	0.056		0.132		0.292		0.499		0.032	
	COEF (SD)	P	COEF (SD)	P	COEF (SD)	P	COEF (SD)	P	COEF (SD)	P
Intercept	3.104 (9.373)	0.326	1.061 (0.207)	**< 0.001**	1.034 (0.193)	**< 0.001**	1.021 (0.164)	**< 0.001**	1.040 (0.261)	**< 0.001**
Slope	-2.124 (9.749)	0.510	0.574 (1.649)	0.303	0.906 (1.577)	0.107	1.850 (2.071)	**0.022**	-0.220 (1.363)	0.623
Green Standing Biomass										
Model	**Kearney Model**		**Model A**		**Model B**		**Model C**		**Model D**	
R-squared	0.644		0.763		0.789		0.889		0.751	
	COEF (SD)	P	COEF (SD)	P	COEF (SD)	P	COEF (SD)	P	COEF (SD)	P
Intercept	52.368 (41.24)	**0.004**	-0.308 (2.574)	0.706	-0.242 (2.372)	0.756	-0.241 (1.668)	0.660	-0.410 (2.694)	0.643
Slope	-5.412 (4.500)	**0.005**	1.424 (.888)	**< 0.001**	1.110 (0.642)	**< 0.001**	1.065 (0.422)	**< 0.001**	1.371 (0.882)	**0.001**

Most models I trained on this landscape turned out to be a better fit to the collected standing biomass than the original Kearney model (Table 9), as would be expected. The models I trained utilizing the same variables as the Kearney model but with site-specific parameter values, entitled Model A, were the least capable of the Sentinel-derived model variations. Model A only had a significant slope when estimating green standing biomass ($p < 0.001$) and accounted for 76.3% of the variation observed in clipped green biomass.

Further, the models utilizing all the variables from the original model in addition to NDVI, Model B, fit variation in observed biomass better than Model A, but were still not the best

fit to my biomass collections (Table 9). I found that only the model B variation built for predicting green biomass had a significant slope ($p < 0.001$).

The models utilizing NDVI as a variable instead of NIR, entitled Model C, captured the most variation in observed biomass (Figure 8, circles). When used to predict green standing biomass, this model accounted for 88.9% of the observed biomass variation (Figure 8B); when utilized for total standing biomass, 49.9% of the observed biomass variation was explained (Figure 8A). Unlike every other model tested over the course of this research, I found Model C to have a statistically significant slopes when this model was used to estimate both total ($p = 0.022$) and green biomass ($p < 0.001$).

The last model variation examined, the Micasense-derived Model D, was built from only NDVI and NIR, and operates the poorest in predicting both kinds of standing biomass in comparison to all other model variations built from this dataset (Table 9). I found that only the variation of this model built for generating predictions of green standing biomass were statistically significant ($p = 0.001$). Figure 8 visualizes the comparison between the original model and that of the most accurate model variation, for both total and green biomass predictions.

Figure 8: Linear regressions of observed VS. predicted for total standing (top panel) and green standing biomass (bottom panel). The 'Kearney' model is shown compared to the best model I developed ('Behnke C').

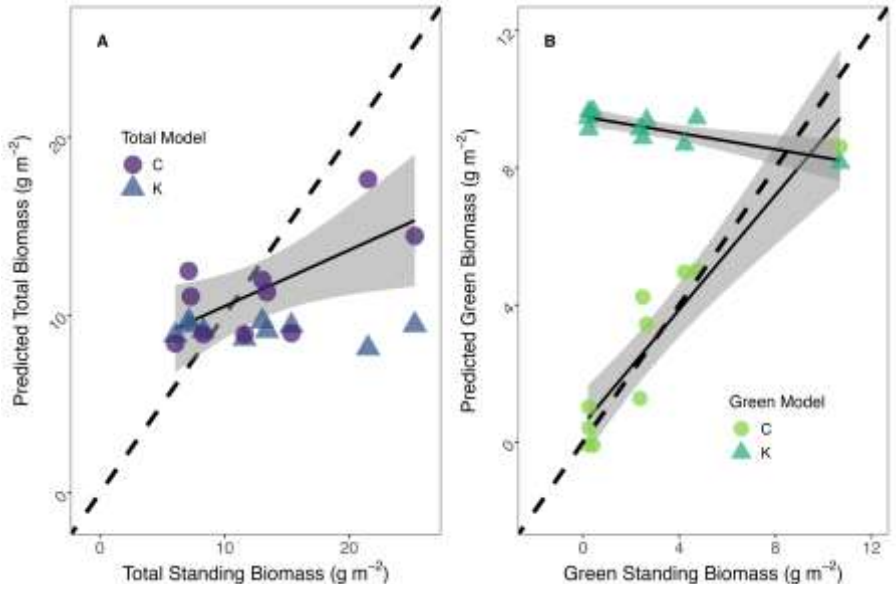

2.4 Discussion

In this study, I tested whether a statistical model trained to estimate plant biomass production from remote imagery in one shortgrass site could be used to predict biomass production in different pasture compositions across nearby rangelands in same region of Colorado. The initial biomass estimations I generated from the base model I tested (referred to as the 'Kearney' model), remote imagery of my site alone did not do a good job of predicting biomass in the pastures of study. Pasture compositions and weather conditions at the site of study were different from those of the site used to train the Kearney model, such that the transferability of the base model to accurately estimate biomass in the pastures of study is apparently limited. The limited transferability is an important constraint to note for anyone utilizing such models, in that site conditions, and more broadly, ecosystem type, should be a major consideration in biomass modeling (Wijesingha et al. 2020). By calibrating the model to the specific conditions at my site, I was able to improve the ability of that model to predict forage. Further, by slightly augmenting the Kearney model variables, in addition to making site-specific calibrations, I generated a yet better fit model for aboveground biomass at the study site. The capacity of the base Kearney model to be improved with site-specific calibrations indicates the opportunity for specializing such models for use in rangeland management. This study demonstrates that any rangeland manager using biomass models to monitor their pastures remotely needs to be aware of the specific constraints of those models, and exercise caution when making inferences from models trained in rangeland systems different from their own.

2.4.1 Biomass Models

Kearney et al. (2022) recently published a model utilizing multispectral imagery from the Harmonized Landsat Sentinel dataset to estimate biomass in a nearby SGS ecosystem (mean absolute error = 151–182 kg ha^{-1}; R^2 = 0.75–0.79), which is dominated by a native C4 grass. The system I studied was in the same climate, but had been planted with naturalized C3 pasture grasses (Crested Wheatgrass and Russian Wildrye), and the site additionally experienced some natural regeneration of rabbitbrush, none of which had been accounted for in the original Kearney model. In addition to the different vegetation types at my site compared to Kearney's SGS site, there were no bulk grazers present for this research as there were at the Kearney site,

only simulations of grazing via mowing standing biomass in the designated treatment plots. Thus, plots not mowed contained much more dead standing biomass than plots used to train the Kearney model would have been.

When applied to the control plots of my study system using Sentinel multispectral bands, the Kearney model did not predict biomass very well across different treatments for total biomass as the slope for the regression did not differ from zero. When the Kearney model was used to estimate only the green biomass at this site, the slope was actually negative. The small differences in band width between the Harmonized dataset and standalone Sentinel dataset could certainly be the source of some of these limitations met by the Kearney model when applied to my research site. The large component of dead biomass from the previous growing season still standing on the landscape could have also contributed to the poor correlation and low slope. Also, the vegetation composition and structure were different between my site and CPER, where the Kearney model was developed. My site was dominated by one of two pasture grasses that are both cool-season bunchgrasses with very dense, distinct bunches; where the original model was trained, the dominant grasses are a mix of warm- and cool-season (*Bouteloua gracilis* and, to a lesser extent, *Pascopyrum smithi)*(Porensky et al. 2017). Although the warm-season grass *B. gracilis* is often considered a bunchgrass, it does not form the same dense and distinct bunches as Russian Wildrye and Crested Wheatgrass, nor does it stand as tall in the landscape or utilize the same photosynthesis pathway (Ogle, 2002). As such, the physical structure of the vegetation as well as the presence of dead biomass could have caused the Kearney model to work less accurately in the system of study (Rigge et al. 2013). An important take-away from this result is that models operate best when trained or calibrated to the specific landscape of use, so rangeland stakeholders should be hesitant to take a biomass model developed in one system and apply it to others without verification that it works (Wijesingha et al. 2020).

I developed three alternative models to evaluate their performance on the vegetation I measured, training each model on half of the dataset and then testing the results on the remaining half. Model A used the same variables as the Kearney model but different coefficient values trained on data from the research site (Table 3). Then Models B and C explored both adding substituting variables in the Kearney model and Model D attempted to fit a simplified version of the Kearney model using the UAV observations (Table 3).

All the models I tested performed better at predicting green biomass only, but when standing dead biomass was included the models explained much less of the variability in standing dead. Depending on the management plan for specific systems, the standing dead biomass could be an important component of the system, and none of these models were able to estimate this biomass well for the vegetation I measured. Additional bands from the satellites and/or detailed information from a previous year would need to be included in order to accurately predict total standing biomass in a situation where some standing dead was left on the landscape.

The results from Model A suggest that the parameters included in the Kearney model can also be used to predict biomass well in a different system, but the coefficient values need to be calibrated for each site. Once calibrated, this site-specific version of the Kearney model explained 76% of the variation in green standing biomass. This suggests that using a common set of parameters across a wide range of pastures may be a useful strategy in predicting biomass with a single model. However, the parameter values would need to be changed, and more work is needed to cross a wider spatial gradient to determine what, about the different systems, causes the parameter values to change and if this can be captured in the model structure to make it more transferable.

The original Kearney model did not include NDVI as a parameter, but when I included NDVI in the models, the predictions improved (Models B and C) for both total standing biomass and green biomass (Table 3). Interestingly, the best model for this system was a model that included NDVI but removed stand-alone NIR (Model C). This may be, in part, because there was very little variation in the height of plants across our plots, and so this parameter did not help in predictions. However, this parameter may be important in a more generalizable model that would be used to capture changes over time and across different vegetation types. The way I quantified the fit of the models was comparing the observed vs. predicted values from the model based on the r^2 value, so these results did not 'penalize' the evaluation criteria for the number of variables included in the model. Therefore, this suggests that including NIR in the models was introducing 'noise' to the predictions rather than providing any explanatory power. More work should be done evaluating the importance of including NIR across broader temporal and spatial scales.

2.4.2 Environmental Conditions and Plant Growth Metrics

Environmental conditions for the 2022 season appeared to be water limited for pasture vegetation based on both the limited greenness and biomass accumulation in every non-irrigated plot as the season progressed without sufficient precipitation events and in the continued growth and greenness of plants in the irrigated pastures. Very little plant growth took place after my initial measurements in all sampling blocks, except the irrigated plot. Individuals across the irrigated plot were able to gain height, fruit, and senesce, but few individuals of study across all other treatments succeeded in fruiting, with none of the Wildrye even progressing into successive phenophases. This suggests that, if more water had been available across the study area, the graminoids in these pastures might otherwise have continued normal growth over the course of the season.

2.4.3 Vegetation Indices

The NDVI I calculated from the 2022 growing season at the Gabbard-Rutledge Property were unlike the NDVI trends typically observed in the SGS (Kearney et al. 2022; Gao et al. 2015). In a 'normal' season, NDVI starts low until the onset of spring, increases to a peak around June, and decreases again into fall, for a relatively convex trend January to December. In such seasons, the maximum index value of satellite-derived NDVI usually falls between 0.3 and 0.4 while the minimum index value settles at about 0.15. However, the NDVI values I generated from Sentinel imagery of this specific growing season showed much less variation, with NDVI values reaching peak in late May, declining through June and July, and increasing again into September. The maximum index values I calculated for the 2022 season from the Sentinel imagery was only 0.16 while the minimum value from the Sentinel-derived index was 0.07. This difference in overall index trend is likely the outcome of climatic stress experienced by forage plants at the Gabbard-Rutledge site during the 2022 season.

When comparing the index built from each multispectral imagery source, I found that the two sources (drone-mounted Micasense Vs. Sentinel satellite) showed similar spectral trends but did not agree on the reflectance of spectra, which is a common finding among comparative studies of this nature (Bansod et al. 2017). While both imaging technologies utilize similar spectral bands, the small differences in bandwidth challenge the ability of the two to be comparable in rangeland use. Indeed, the wavelengths employed by the Micasense cameras indexed so much more so than those employed by Sentinel sensors that I found the indices to be significantly different on most passing dates. Because of this significant difference I would not

assume it appropriate to use these imaging technologies interchangeably when imaging landscapes such as the SGS. Both multispectral imaging technologies come with their own advantages and challenges that should be evaluated based on the needs of the model.

2.5 Conclusions

2.5.1 Key Take-aways

Monitoring pastures with remote sensing technologies can provide insights into vegetation conditions such as visual greenness, biomass accumulation, and photosynthetic capacity. Both technologies tested herein (Sentinel and Micasense) have spectral bands that can provide metrics that correlate with and quantify these conditions with varied success. Sentinel spectral products can provide a broader range of bands relevant to vegetation quantification, providing the information from which to extrapolate finer detail in vegetation condition. Meanwhile, Micasense spectral products can capture detail to a much finer spatial scale, giving insight specific to conditions within each pasture. As such, both technologies can prove useful in the monitoring and management of SGS rangelands.

Biomass modeling is not one-size-fits-all. This study shows that two sites that seem relatively similar, or near in geography, can still yield vastly different indices and thus different predictions. The poor fit of the Kearney model in predicting biomass in this study's rangeland system is largely because that model was not calibrated for this specific rangeland system. Differences in any number of factors such as weather conditions, vegetation height, pasture composition (C3 vs C4 plants), and even the presence of grazers in the rangeland systems could have impacted the results of the biomass modeling predictions. For this reason, models should always be employed with consideration to the context of their origin. For rangeland managers using models in ARM decisions, caution to these constraints is key.

2.5.2 Limitations

As with all research, any inferences made from this study come with a variety of limitations. As for my research design, my analysis is limited by a relatively small sample size, having utilized just two pastures at a single site, over the course of a single growing season, and includes only two of the forage species present, one representing each pasture composition. One of the three treatments I tested had no replicates, and the remaining treatments and controls only had three replicates each. As such, this design did not provide a large or broad dataset from

which to train biomass models. In this design, each treatment proxied a changing condition of working rangelands (such as grazing and rain events; to utilize cattle for these grazing treatments or to have received measurable rainfall instead of late season irrigation would have offered more defensible insights into rangeland management applications of remote imagery. Further, the plot setup I utilized did not fully limit pixel overlap for the largest pixels used from the satellite imagery, so the size and lack of distance between plots could have reduced the accuracy of models utilizing satellite imagery in this study. The extreme weather conditions encountered in this study hindered the growth of vegetation across the research site, which also limited the range of pasture conditions I was able to observe and did not make for an excellent dataset for training/testing models. Lastly, the spectral bands used in this research were not of the exact same dataset as used in the original Kearney biomass model. In this research I used the Sentinel dataset, while the Kearney model was trained with the Harmonized Landsat-Sentinel dataset. Small differences in spectral ranges of multispectral bands between those datasets could thus have unforeseen impacts to my testing of the Kearney model as intended.

2.5.3 Future Directions

Further research into the capabilities of these remote monitoring technologies is yet needed to clarify the relationships between spectral reflectance and conditions of vegetation in shortgrass rangelands. For this research, I did not include additional variables accounting for pasture composition/height, as was included in the referenced study (Kearney et al. 2022) among others; the inclusion of such a variables in biomass modeling is one space of further investigation. Future projects studying the application of biomass models might also consider the role of local temperature and moisture conditions for air as well as soil, outside of variables derived solely from imagery. Other imaging technologies such as improved drone-mounted cameras that include the previously-lacking SWIR2 band are also worth future investigation in biomass modeling. Additionally, rangeland biomass models would benefit from training over multiple growing seasons, including full phenological cycles and a wide variety of weather conditions, over the model predictions generated with this study with a single droughted season of data from which to train. A broader timescale and more diverse variety of shortgrass rangelands might allow for better model training. Lastly, this study was not intended to be a comprehensive comparison of all available spectral combinations useful to rangeland management. Additional testing of different spectral combinations, specifically those utilizing

NIR or SWIR bands, could yet benefit biomass prediction models. Any of these options could help inform remote monitoring technologies, such as biomass modeling, for rangeland managers.

LITERATURE CITED

Allen, C. R., Angeler, D. G., Fontaine, J. J., Garmestani, A. S., Hart, N. M., Pope, K. L., and D. Twidwell. 2017. Adaptive management of rangeland systems. In Rangeland Systems: Processes, Management and Challenges, pp. 373-394. Springer.

Arzani, H., Ahmadi, Z., Azarnivand, H., and M.R. Bihamta. 2010. Forage quality of three life forms of rangeland species in semi-arid and semi-humid regions in different phenological stages. Desert, 15.

Arzani, H., Zohdi, M., Fish, E., Amiri, G. Z., Nikkhah, A., & Wester, D., 2004. Phenological effects on forage quality of five grass species. Journal of Range management, 57(6), 624-629.

Augustine, D.J. 2010. Spatial versus temporal variation in precipitation in a semiarid ecosystem. Landsc. Ecol. 25, 913–925. https://doi.org/10.1007/s10980-010-9469-y.

Axelrod, D. I., 1985. Rise of the grassland biome, central North America. The Botanical Review, 51(2), 163–201. https://doi.org/10.1007/BF02861083.

Barr, H. D., & Weatherley, P. E., 1962. A re-examination of the relative turgidity technique for estimating water deficit in leaves. Aust. J. Biol. Sci., 15, 413-428.

Bansod, B., Singh, R., Thakur, R. and Singhal, G. 2017. A comparision between satellite based and drone based remote sensing technology to achieve sustainable development: a review. Journal of Agriculture and Environment for International Development (JAEID). 111, 2 (Dec. 2017), 383–407. https://doi.org/10.12895/jaeid.20172.690.

Blair, J., Nippert, J., and J. Briggs. 2014. Grassland ecology. In Ecology and the Environment, pp. 147-164. Springer. https://doi.org/10.1007/978-1-4614-7501-9_14.

Borowik, T., Pettorelli, N., Sönnichsen, L., and B. Jędrzejewska. 2013. Normalized difference vegetation index (NDVI) as a predictor of forage availability for ungulates in forest and field habitats. European journal of wildlife research, 59(5), 675-682.

Brakie, M. R., 2013. Plant Guide for buffalograss, Bouletoua dactyloides (Nutt.) J.T. Columbus. USDA Natural Resources Conservation Service, East Texas Plant Materials Center, Nacogdoches, TX 75964.

Briske, D. D., Ritten, J. P., Campbell, A. R., Klemm, T., and A.E. King. 2021. Future climate variability will challenge rangeland beef cattle production in the Great Plains. Rangelands, 43(1), 29-36.

Browning, D. M., Snyder, K. A., and J.E. Herrick. 2019. Plant phenology: taking the pulse of rangelands. Rangelands, 41(3), 129-134.

Browning, D.M., Russell, E.S., Ponce-Campos, G.E., Kaplan, N., Richardson, A.D., Seyednasrollah, B., ... and S.D. Taylor. 2021. Monitoring agroecosystem productivity and phenology at a national scale: A metric assessment framework. *Ecological Indicators*, *131*, 108147.

Copernicus Sentinel-2A Multispectral Imagery. 2022. Retrieved from the Copernicus SciHub, via the European Space Agency.

Cox, C., 2006. US Agriculture conservation policy and programs: History, trends, and implications. US Agricultural Policy and the 2007 Farm Bill, p.3.

Denny, E.G., Gerst, K.L., Miller-Rushing, A.J., Tierney, G.L., Crimmins, T.M., Enquist, C.A., Guertin, P., Rosemartin, A.H., Schwartz, M.D., Thomas, K. A., and J.F. Weltzin. 2014. Standardized phenology monitoring methods to track plant and animal activity for science and resource management applications. International journal of biometeorology, 58(4), 591–601. https://doi.org/10.1007/s00484-014-0789-5

Derner, J.D. and D.J. Augustine. 2016. Adaptive management for drought on rangelands. Rangelands, *38*(4), pp.211-215.

Derner, J.D., Augustine, D.J., Briske, D.D., Wilmer, H., Porensky, L. M., Fernández-Giménez, M. E., ... and J.P. Ritten. 2021. Can collaborative adaptive management improve cattle production in multipaddock grazing systems?. Rangeland Ecology & Management, 75, 1-8.

Derner, J. D., Budd, B., Grissom, G., Kachergis, E. J., Augustine, D. J., Wilmer, H., ... and J.P. Ritten. 2022. Adaptive grazing management in semiarid rangelands: An outcome-driven focus. Rangelands, 44(1), 111-118.

Epstein, H. E., Lauenroth, W. K., and I.C. Burke. 1997. Effects of Temperature and Soil Texture on ANPP in the U.S. Great Plains. Ecology, 78(8), 2628–2631. https://doi.org/10.2307/2265921

Esri Inc., 2023. ArcGIS Pro (version 3.1.1). Software. Redlands, CA: Esri Inc.

European Space Agency, 2018. MultiSpectral Instrument (MSI) Overview. Sentinel Online.

Gucker, C.L., and N.L. Shaw. 2018. Scarlet globemallow (Sphaeralcea coccinea) In: eds. Western forbs: Biology, ecology, and use in restoration. Reno, NV: Great Basin Fire Science Exchange.

Hardisky, M.A., Klemas, V. and R.M. Smart. 1983. The Influence of Soil Salinity, Growth Form, and Leaf Moisture on the Spectral Radiance of Spartina alterniflora Canopies. Photogrammetric Engineering and Remote Sensing, 49, 77-83.

Havstad, K., Peters, D., Allen-Diaz, B., Bartolome, J., Bestelmeyer, B., Briske, D., Brown, J., Brunson, M., Herrick, J., Huntsinger, L., Johnson, P., Joyce, L., Pieper, R., Svejcar, T. and J. Yao. 2009. The Western United States Rangelands: A Major Resource. In Grassland Quietness and Strength for a New American Agriculture (eds W.F. Wedin and S.L. Fales). https://doi.org/10.2134/2009.grassland.c5

Havstad, K.M., Peters, D.P., Skaggs, R., Brown, J., Bestelmeyer, B., Fredrickson, E., Herrick, J. and J. Wright. 2007. Ecological services to and from rangelands of the United States. Ecological Economics, 64(2), pp.261-268.

Heitschmidt, R.K. and J.W. Stuth. 1991. Grazing Management: An Ecological Perspective. Portland, OR: Timber Press. https://cnrit.tamu.edu/rlem/textbook/textbook-fr.html

IPCC, 2022. Climate Change 2022: Impacts, Adaptation, and Vulnerability. Contribution of Working Group II to the Sixth Assessment Report of the Intergovernmental Panel on Climate Change. Pörtner, H.O., Roberts, D.C., Tignor, M., Poloczanska, E.S., Mintenbeck, K., Alegría, A., Craig, M., Langsdorf, S., Löschke, S., Möller, V., Okem, A., Rama, B. (eds.). Cambridge University Press. (In Press).

Irisarri, J.G.N., Durante, M., Derner, J.D., Oesterheld, M. and J.D. Augustine. 2022. Remotely sensed spatiotemporal variation in crude protein of shortgrass steppe forage. Remote Sensing, 14(4), p.854.

Johnson, H., Gustine, D., Golden, T., Adams, L., Parrett, L., Lenart, E. and P. Barboza. 2018. NDVI exhibits mixed success in predicting spatiotemporal variation in caribou summer forage quality and quantity. Ecosphere, 9(10), p.e02461. https://doi.org/10.1002/ecs2.2461

Jones, M.O., Robinson, N.P., Naugle, D.E., Maestas, J.D., Reeves, M.C., Lankston, R.W., B.W. Allred. 2021. Annual and 16-day rangeland production estimates for the Western United States. Rangel. Ecol. Manag. 77, 112–117.

Joyce, L.A. and N.A. Marshall. 2017. Managing climate change risks in rangeland systems. In: Rangeland Systems: Processes, Management, and Challenges, pp. 491-526.

Joyce, L.A., Ojima, D., Seielstad, G.A., Harriss, R. and J. Lackett. 2001. Potential consequences of climate variability and change for the Great Plains. In: Climate Change Impacts on the United States: The Potential Consequences of Climate Variability and Change, pp. 191-217. Available at: http://www.climateimpacts.org/us-climate-assess-2000/synthesis-reports/foundation/07GP.pdf

Karl, J.W., Herrick, J.E. and D.A. Pyke. 2017. Monitoring protocols: options, approaches, implementation, benefits. In: Rangeland Systems: Processes, Management, and Challenges, pp. 527-567.

Kearney, S.P., Porensky, L.M., Augustine, D.J., Derner, J.D. and F. Gao. 2021. Predicting spatial‐temporal patterns of diet quality and large herbivore performance using satellite time series. Ecological Applications, 32(2), p.e2503.

Kearney, S.P., Porensky, L.M., Augustine, D.J., Gaffney, R. and J.D. Derner. 2022. Monitoring standing herbaceous biomass and thresholds in semiarid rangelands from harmonized Landsat 8 and Sentinel-2 imagery to support within-season adaptive management. Remote Sensing of Environment, 271, p.112907.

Kukal, M.S. and S. Irmak. 2018. Climate-driven crop yield and yield variability and climate change impacts on the US Great Plains agricultural production. Scientific Reports, 8(1), pp.1-18.

Lauenroth, W.K. and I.C. Burke. 2008. Ecology of the Shortgrass Steppe: A Long-term Perspective. Oxford University Press.

Lauenroth, W.K., Burke, I. and M. Gutmann. 1999. The Structure and Function of Ecosystems in the Central North American Grassland Region. Great Plains Research, 9, pp.223-259.

Lauenroth, W., Burke, I. and J. Paruelo. 2000. Patterns of Production and Precipitation-Use Efficiency of Winter Wheat and Native Grasslands in the Central Great Plains of the United States. Ecosystems, 3, pp.344-351. https://doi.org/10.1007/s100210000031

Lauenroth, W.K. and D.G. Milchunas. 1991. Shortgrass steppe. In: R.T. Coupland, ed., Natural Grasslands: Introduction and Western Hemisphere. Volume SA. Ecosystems of the World. Elsevier, pp.183-226.

Lauenroth, W.K. and O.E. Sala. 1992. Long-term forage production of North American shortgrass steppe. Ecological Applications, 2(4), pp.397-403.

Main-Knorn, M., Pflug, B., Louis, J., Debaecker, V., Müller-Wilm, U. and F. Gascon. 2017. Sen2Cor for sentinel-2. In Image and Signal Processing for Remote Sensing XXIII (Vol. 10427, pp. 37-48). SPIE.

McCollum, D.W., Tanaka, J.A., Morgan, J.A., Mitchell, J.E., Fox, W.E., Maczko, K.A., Hidinger, L., Duke, C.S. and U.P. Kreuter. 2017. Climate change effects on rangelands and rangeland management: affirming the need for monitoring. *Ecosystem Health and Sustainability*, *3*(3), p.e01264.

Milchunas, D.G., Sala, O.E. and W.K. Lauenroth. 1988. A generalized model of the effects of grazing by large herbivores on grassland community structure. The American Naturalist, 132(1), pp.87-106.

Moore, L.M., Lauenroth, W.K., Bell, D.M. and D. R. Schlaepfer. 2015. Soil water and temperature explain canopy phenology and onset of spring in a semiarid steppe. *Great Plains Research*, pp.121-138.

National Agricultural Statistical Service, USDA. 2019. 2017 Census of Agriculture (AC-17-A-51). Available at: https://www.nass.usda.gov/Publications/AgCensus/2017/Full_Report/Volume_1,_Chapter_1_US/usv1.pdf

Ogle, D. 2002. USDA-NRCS Plant Guide: blue grama, Bouteloua gracilis (Willd. ex Kunth.) Lag. Ex-Griffiths. Washington, DC, USA: USDA-NRCS.

Ogle, D., St. John, L. and J. B. Jensen. 2006. USDA-NRCS Plant Guide: Crested Wheatgrass, *Agropyron cristatum* (L.) Gaertn. Washington, DC, USA: USDA-NRCS.

Ogle, D., St. John, L. and S. Winslow. 2000. USDA-NRCS Plant Guide: western wheatgrass, *Pascopyrum smithii* (Rydb.) A. Love. Washington, DC, USA: USDA-NRCS.

Ogle, D., St. John, L., Cornwell, J., Holzworht, L., Majerus, M., Tober, D., Jensen, K. and K. Sander. 2004. USDA-NRCS Plant Guide: Russian wildrye, *Psathyrostachys junceus* (Fisch.) Nevski. Washington, DC, USA: USDA-NRCS.

Ogle, D., St John, L. and K. Jensen. 2010. Species selection and grazing management guidelines. Pasture and grazing management in the Northwest, PNW, 614, pp.7-20.

O'Mara, F.P. 2012. The role of grasslands in food security and climate change. Annals of botany, 110(6), pp.1263-1270.

Otfinowski, R., Kenkel, N.C. and P.M. Catling. 2007. The biology of Canadian weeds. 134. *Bromus inermis* Leyss. Canadian Journal of Plant Science, 87(1), pp.183-198.

Pettorelli, N., Vik, J.O., Mysterud, A., Gaillard, J.M., Tucker, C.J. and N.C. Stenseth. 2005. Using the satellite-derived NDVI to assess ecological responses to environmental change. Trends in ecology & evolution, 20(9), pp.503-510.

Porensky, L.M., Derner, J.D., Augustine, D.J. and D.G. Milchunas. 2017. Plant community composition after 75 yr of sustained grazing intensity treatments in shortgrass steppe. Rangeland Ecology & Management, 70(4), pp.456-464.

R Core Team. 2023. R: A Language and Environment for Statistical Computing. R Foundation for Statistical Computing, Vienna, Austria.Statistical Computing, Vienna, Austria.

Rigge, M., Smart, A., Wylie, B., Gilmanov, T. and P. Johnson. 2013. Linking Phenology and Biomass Productivity in South Dakota Mixed-Grass Prairie Natural Resource Management Faculty Publications, 288.

Robinson, N.P., Allred, B.W., Jones, M.O., Moreno, A., Kimball, J.S., Naugle, D.E., ... and A.D. Richardson. 2017. A dynamic Landsat derived normalized difference vegetation index (NDVI) product for the conterminous United States. Remote sensing, 9(8), 863.

Rouse Jr, J.W., Haas, R.H., Schell, J.A. and D.W. Deering. 1973. Monitoring the vernal advancement and retrogradation (green wave effect) of natural vegetation (No. NASA-CR-132982).

Sala, O.E., Parton, W.J., Joyce, L.A., and W.K. Lauenroth. 1988. Primary production of the central grassland region of the United States. Ecology, 69(1), 40-45.

Sala, O.E., Yahdjian, L., Havstad, K. and M.R. Aguiar. 2017. Rangeland ecosystem services: Nature's supply and humans' demand. In: D. Briske, ed., Rangeland systems: Processes, management, and challenges, pp.467-489.

Skold, M.D. 1989. Cropland Retirement Policies and Their Effects on Land Use in the Great Plains. *Journal of Production Agriculture, 2*, 197-201.

Soil Survey Staff, Natural Resources Conservation Service, United States Department of Agriculture (NRCS, USDA). 2013. Larimer County Area, Colorado (Gabbard-Ruttledge Property) Web Soil Survey. National Cooperative Soil Survey. Available online. Accessed [02/08/2013].

Taliga, C.E. and S. Parr. 2012. Plant fact sheet for Prairie sage (*Artemisia frigida*). USDA-Natural Resources Conservation Service, Denver State Office. Denver, Colorado.

Tilley, D. and L. St. John. 2012. Plant Guide for yellow rabbitbrush (*Chrysothamnus viscidiflorus*). USDA-Natural Resources Conservation Service, Aberdeen Plant Materials Center. Aberdeen, Idaho 83210.

U.S. Department of Agriculture (USDA). 2004. 2002 Farm Bill–Conservation Reserve Program long-term policy; Interim rule: Farm Service Agency, Commodity Credit Corporation: Federal Register, v. 68, no. 89, p. 24830–24845.

Watson, C.J., Restrepo-Coupe, N., and A.R. Huete. 2019. Multi-scale phenology of temperate grasslands: Improving monitoring and management with near-surface phenocams. *Frontiers in Environmental Science*, *7*, p.14.

Weiss, W.P. and M.B. Hall. 2020. Laboratory methods for evaluating forage quality. In: G.C. Fahey and L.H. Pennington, eds., Forages: The Science of Grassland Agriculture, 2, pp.659-672.

Wijesingha, J.T., Schulze-Brüninghoff, D., Wengert, M., and M. Wachendorf. 2020. Predicting Forage Quality of Grasslands Using UAV-Borne Imaging Spectroscopy. Remote Sensing, 12(1), p.126. https://doi.org/10.3390/rs12010126

Zhang, T., Su, J., Liu, C., Chen, W.H., Liu, H., and G. Liu. 2017. Band selection in sentinel-2 satellite for agriculture applications. In 2017 23rd international conference on automation and computing (ICAC) (pp. 1-6). IEEE.

Appendix

Supplemental Figure 1: Single research plot example map, applicable to each of the 20 unique plots utilized in the course of this project. Plots measured 30x30m with insets measuring 20x20 m, leaving a 5 m buffer zone around each inset. Each inset contained four plants, either Russian Wildrye or Crested Wheatgrass depending on pasture, which I selected based on the plant's location along a diagonal transect.

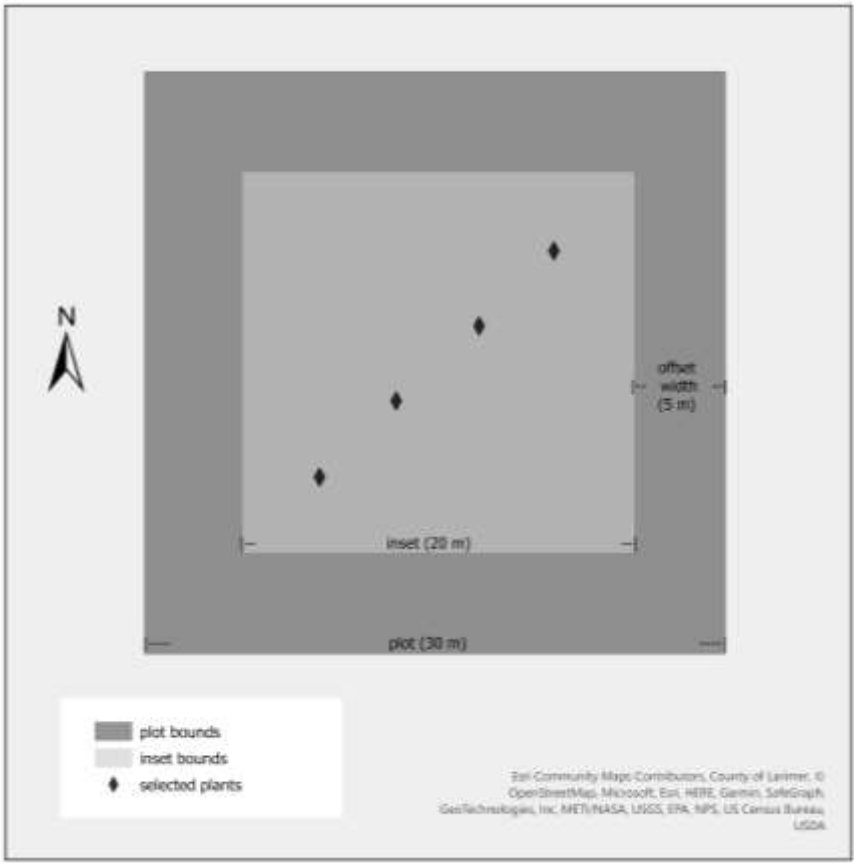

Supplemental Table 1: List of spectral bands of interest and spatial resolution. Micasense bands RED1 (B5) and RED2 (B6) were used together to cover wavelength range more comparable to Sentinel's RED (B4).

Spectra Source	Band	Range (nm)	Center Wavelength	Pixel Size (m)
Sentinel	GREEN (B3)	542-577	560	30
Micasense	RED1 (B5)	642-658	650	0.067
Micasense	RED2 (B6)	663-673	665	0.067
Sentinel	RED (B4)	649-680	665	10
Micasense	NIR (B10)	820-860	840	0.067
Sentinel	NIR (B8A)	855-875	865	20
Sentinel	SWIR2 (B12)	2215-2290	2190	20

Table 2: Model variable coefficients built from observations of total above-ground biomass. Kearney Model, as well as Behnke Models A, B, and C, sourced from Sentinel 2A MSI 2A data; Behnke Model D sourced from Micasense data.

Model	Kearney HLS-only Model	Behnke Model A	Behnke Model B	Behnke Model C	Behnke Model D
Variable	**COEF**	**COEF (SE)**	**COEF (SE)**	**COEF (SE)**	**COEF (SE)**
Intercept	20.161	-185.040 (172.735)	-302.560 (206.570)	-111.692 (132.650)	-14.820 (28.550)
NDII7	16.704	111.037 (89.0178)	147.570 (95.500)	185.377 (92.859)	-
NDVI	-	-	-205.490 (200.130)	-217.878 (206.294)	-65.440 (49.110)
BAI	-0.059	0.976 (0.810)	1.930 (1.230)	1.100 (1.042)	-
NIR	-0.005	188.564 (153.280)	180.330 (152.800)	-	184.110 (106.95)

Table 7: Model variable coefficients built from unaltered observations of green above-ground biomass. Kearney Model, as well as Behnke Models A, B, and C, sourced from Sentinel 2A MSI 2A data; Behnke Model D sourced from Micasense data. Model coefficients for the Kearney model are from published data and so we were not able to calculate the SE of these values.

Model	Kearney HLS-only Model	Behnke Model A	Behnke Model B	Behnke Model C	Behnke Model D
VARIABLE	**Coefficients (SE)**				
Intercept	20.161	11.595 (43.761)	-41.332 (38.616)	-95.084 (28.198)	-8.845 (15.034)
NDII7	16.704	33.935 (22.552)	50.389 (17.852)	39.742 (19.613)	-
NDVI	-	-	-92.546 (37.413)	-89.056 (43.573)	34.192 (25.863)
BAI	-0.059	0.060 (0.205)	0.490 (0.230)	0.723 (0.220)	-
NIR	-0.005	-47.078 (38.832)	-50.786 (28.565)	-	18.400 (56.328)

Supplemental Figure 2: Stretch plant height (shown in cm) for each treatment over time, represented as boxplots. The top panel contains the heights measured in the wheatgrass plots; the bottom panel contains heights measured in the wildrye plots. Treatment events of mowing (green dashed line) and irrigation (blue dotted line) are indicated by vertical lines. Treatments are indicated by color.